Theoretical and Computational Neuroscience: Collective Dynamics of Biological Neural Networks II

taught by

Prof. Dr. Fred Wolf

Georg-August-Universität Göttingen
Göttingen, Niedersaschen, Deutschland
Sommer (SoSe) 2021

Compiled by Neil Wesch

Last edited on 22 July 2021

Contents

Chapter 1

Neuronal Excitability

Neurons communicate with each other using the digital language of action potentials. These spikes are unitary events which travel through the axon and interact with other directly connected neurons. All of the internal degrees of freedom of a neuron are biophysical variables, such as ionic concentrations and trans-membrane potential. The synapses translate these continuous internal variables of single cell biophysics into sequences of spikes.

Information is not primarily conveyed by the individual activity of single cells but rather signals from small populations of cells in neuronal ensembles. A typical neuron fires at approximately 1 $[Hz]$, although this varies. Assuming heterogeneous firing, this means in a collection of 1000 neurons a new spike occurs every 1 $[ms]$. At this level, the important quantity is the time-dependent population firing rate $\nu(t)$.

The laws of motion for the dynamical variables describe a neuron, equivalent to any classical physical system. The typical conductance based model (Hodgkin-Huxley) is a standard way to describe the interplay of ion channel activation. Ion channels are the main sources of current through the membrane and they interact through the single variable of membrane potential $V(t)$. The kinetic equations which describe the opening and closing of ion channels are built on models of gating variables.

1.1 Biophysics of Spike Generation

The biophysical structures responsible for membrane excitability are ion channels and the electronic charge carriers are ions: Na^+, K^+, Ca^{2+}. These ion channels are embedded in a lipid membrane, which due to its low permeability to ions maintains charge seperation across the membrane; therefore acting like a capacitor. Ion channels play the role of selective voltage-gated holes which mediate the transfer of ions from inside/outside the neuron.

1.1.1 Ion Channel Dynamics

At the biomolecular level ion channels undergo conformation changes from an 'open' to a 'closed' state. The activity of a neuron is dictated by state transitions from open to closed, which is dependent on physical variables such as membrane potential. This process is *Markovian* in that only the present state affects the future state.

The total current through the ion channels will depend on the:

- probability that the j^{th} species (e.g. sodium, potassium) of ion channel is in an *open* state rather than a *closed* state - P_j
- total number of j^{th} type ion channels - N_j
- average conductance of the j^{th} type ion channels - $\bar{g}_j$
- difference between the membrane potential $V(t)$ and the reversal potential of the j^{th} species $\bar{V}_j$, termed the *driving force* - $[V(t) - \bar{V}_j]$

Collectively the current for the j^{th} species of ion is described by Eqn (1.1a), where the probability of a single ion channel being open is given by the master equation Eqn (1.1b), with opening $\alpha(V)$ and closing $\beta(V)$ transition rates.

$$I_j(t) = P_j N_j g_j [V(t) - \bar{V}_j] \tag{1.1a}$$

$$P_j(t) = \alpha(V)[1 - P_j(t)] - \beta(V)P_j(t) \tag{1.1b}$$

This simplified case, where ion channels only have two states, is schematically shown in Fig 1.1(top). However, real ion channels have multiple closed states as depicted in Fig 1.1(bottom). Note that this is a *Markov chain* process.

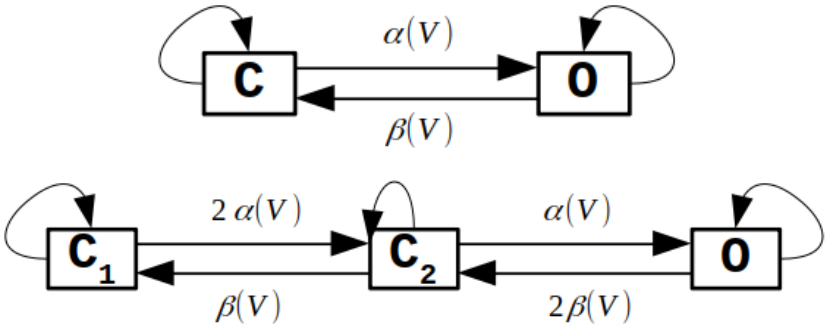

Figure 1.1: Schematic representation of ion channel transitions from closed C to open O states; the opening rate $\alpha(V)$ and closing rate $\beta(V)$ are voltage-dependent. **(top)** A two-state system, **(bottom)** a three-state system with two different closed states C_1, C_2.

The opening and closing of ion channels is not an instantaneous process. Gating variables with characteristic time constants are used to describe the voltage-dependent flow of ions. A gating variable, x, which describes the opening of a channel is termed an *activation variable*. The probability that an ion channel is open can be expressed as a function of these gating variables $P_j(t) = x^y$ where y is the number of closed states. (This is valid assuming complete symmetry between closed states and transition rates.)

1.1.2 Gating Variables

Associated with the passing of Na^+ through voltage-gated Na_V channels are the *activation variable* $m(t)$ and *inactivation variable* $h(t)$. Similarly for K^+ through K_V channels is the *activation variable* $n(t)$. A spike is elicited based upon the in-step time-evolution of these three gating variables - when they are large the respective ion channels have a large probability of being open, causing ionic currents to cross the membrane.

At the moment of action potential generation, $m(t)$ almost instantly increases from zero to unity, plateaus, then almost instantly returns to zero. This corresponds to the activation of the sodium current, as Na^+ rushes into the cell. With a small time lag the sodium inactivation gating variable $h(t)$ increases, reaching a maximum at the downstroke of $m(t)$ - together these create a sharp increase in membrane potential (the spike) and an abrupt stop to I_{Na}.

The potassium activation variable follows the same time course, but with mirrored values, beginning near zero at the time of sodium current cessation and increases mono-

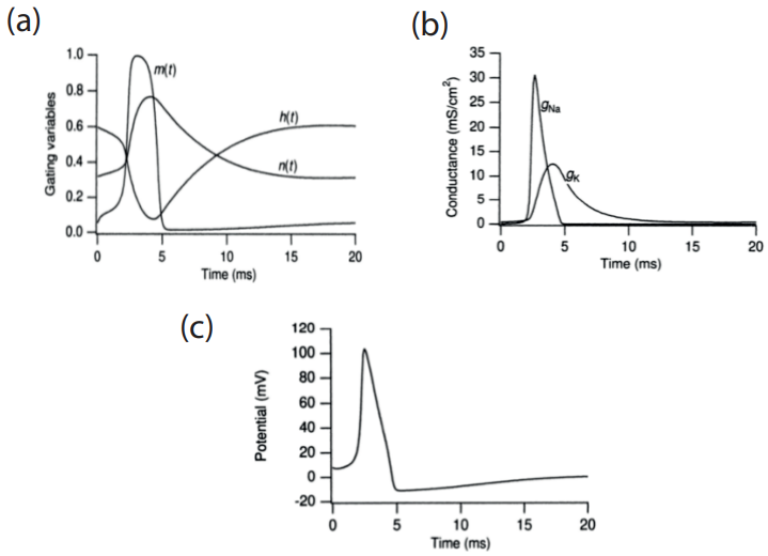

Figure 1.2: **(a)** Time dependence of gating variables m, n, h during an action potential and **(b)** the resulting time-dependent changes to the sodium and potassium conductances. **(c)** The resulting membrane potential $V(t)$ during a spike. Adapted from "Dynamical Systems in Neuroscience" by E. M. Itzhikevich [1]

tonically. Physically this is realized by K^+ exiting the cell and returning the membrane voltage to its pre-spike level. The I_K actually overshoots (based on its different reversal potential to sodium) which causes the neuron to hyperpolarize and results in a post-spike refractory period. This is shown in Fig 1.2a,c.

Each of these gating variables and their time constants are voltage-dependent. Figure 1.3 shows the voltage-dependent steady-state values $m_\infty(V), h_\infty(V), n_\infty(V)$ (left) and the time constants $\tau_m(V), \tau_h(V), \tau_n(V)$ (right).

The intrinsic dynamics of ion channels are stochastic therefore voltage-dependent opening and closing rates, $\alpha_x(V)$ and $\beta_x(V)$, are used to describe the transition from one state to the other. Explicitly, the set of equations which describe the *excitation dynamics* are

$$\dot{m}(t) = \alpha_m(V)[1 - m(V)] - \beta_m(V)m(t) \tag{1.2a}$$

$$\dot{h}(t) = \alpha_h(V)[1 - h(V)] - \beta_h(V)h(t) \tag{1.2b}$$

$$\dot{n}(t) = \alpha_n(V)[1 - n(V)] - \beta_n(V)n(t) \tag{1.2c}$$

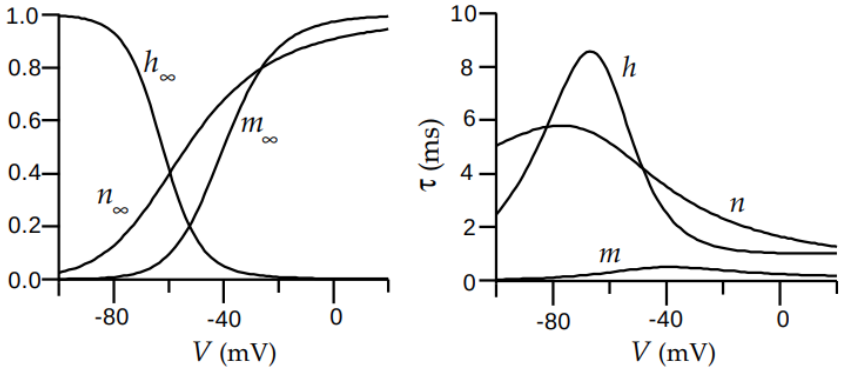

Figure 5.10 The voltage-dependent functions of the Hodgkin-Huxley model. The left panel shows $m_\infty(V)$, $h_\infty(V)$, and $n_\infty(V)$, the steady-state levels of activation and inactivation of the Na^+ conductance, and activation of the K^+ conductance. The right panel shows the voltage-dependent time constants that control the rates at which these steady-state levels are approached for the three gating variables.

Figure 1.3: Taken from "Theoretical Neuroscience" by P. Dayan and L.F. Abbott [2]

Letting x represent m, h, n the general expression for each time constant in terms of stochastic opening and closing rates is given by

$$\tau_x(V) = \frac{1}{\alpha_x(V) + \beta_x(V)} \tag{1.3}$$

Introducing equilibrium (or steady state) values of the gating variables, in terms of stochastic opening and closing rates

$$x_\infty(V) = \frac{\alpha_x(V)}{\alpha_x(V) + \beta_x(V)} \tag{1.4}$$

allows for the gating variable dynamics to be equivalently expressed as

$$\tau_x(V)\dot{x}(t) = x_\infty(V) - x(t) \tag{1.5}$$

The overall dynamics of the membrane voltage, gating variables, conductances, and ionic currents in response to two external square impulse currents is depicted in Fig 1.4.

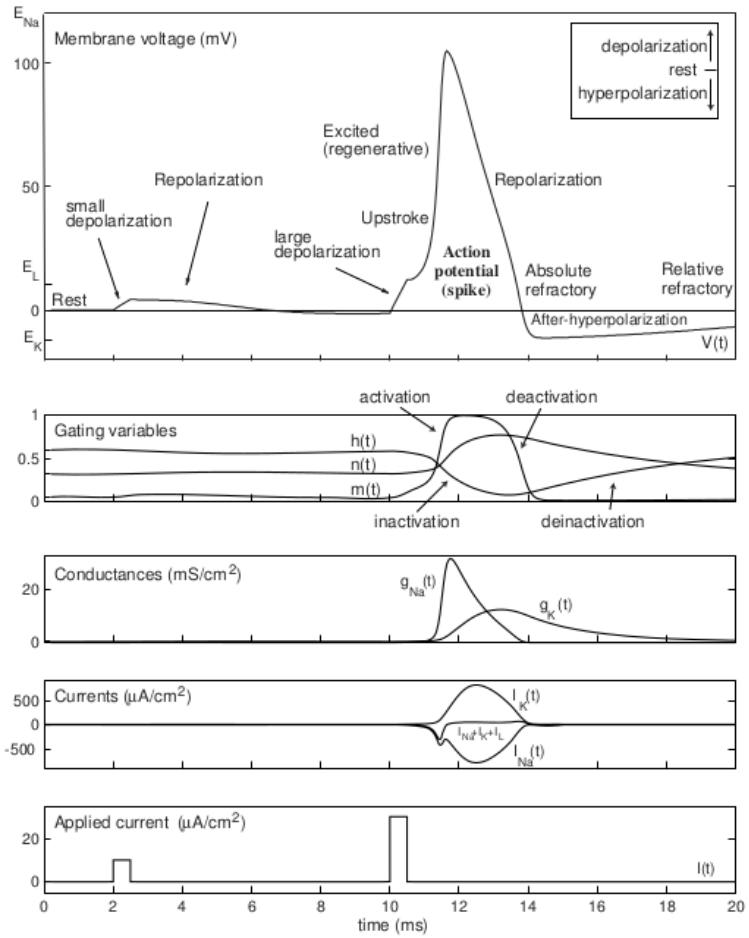

Figure 2.15: Action potential in the Hodgkin-Huxley model.

Figure 1.4: Taken from "Dynamical Systems in Neuroscience" by E. M. Itzhikevich [1]

Boltzmann Distribution

For the simple case of two non-degenerate states with an energy level difference ΔE the opening rate will depend on the Boltzmann factor

$$\alpha(V) \sim e^{-\Delta E/k_B T} \qquad \Delta E \sim V \tag{1.6}$$

The energy change is proportional to electric field which is dependent on change in voltage across the membrane. Letting $V_{1/2}$ denote the *half-activation voltage* the canonical

choice for activation variables and timescales is

$$x_\infty = \frac{1}{1 + e^{-(V - V_{1/2})/k_B T}} \tag{1.7a}$$

$$\tau(V) = \frac{1}{e^{-V/k_B T} + e^{V/k_B T}} \tag{1.7b}$$

A different choice is to neglect the voltage dependence of timescales and assume a typical timescale of activation τ as is done in § 1.1.4.

1.1.3 Power Law Dependence of $P_j(t)$

By fitting gating variables of this form to electrophysiology measurements performed on the squid giant axon, Hodgkin and Huxley concluded that (with $N_j \bar{g}_j = g_j$)

$$P_{Na} = m^3 h \quad \longrightarrow \quad I_{Na}(t) = g_{Na} m^3 h [\bar{V}_{Na} - V(t)] \tag{1.8a}$$

$$P_K = n^4 \quad \longrightarrow \quad I_K(t) = g_K n^4 [\bar{V}_K - V(t)] \tag{1.8b}$$

Therefore the total ionic current across the cell membrane is described by

$$I_{ionic}(t) = I_{Na}(t) + I_K(t) + I_L(t) \tag{1.9a}$$

$$= g_{Na} m^3 h [\bar{V}_{Na} - V(t)] + g_K n^4 [\bar{V}_K - V(t)] + g_L [\bar{V}_L - V(t)] \tag{1.9b}$$

Expressing the trans-membrane current $I_{mem}(t) = C\dot{V}(t)$ gives the *HH equation of motion for the membrane potential of a neuron*

$$C\frac{dV(t)}{dt} = I_{ionic}(t) + I_{ext}(t) \tag{1.10a}$$

$$= g_{Na} m^3 h [\bar{V}_{Na} - V(t)] + g_K n^4 [\bar{V}_K - V(t)] + g_L [\bar{V}_L - V(t)] + I_{ext}(t) \tag{1.10b}$$

Here the $g_L[\bar{V}_L - V(t)]$ is the leak term which accounts for the ever-present *leak current* which arises because of passive ion movement through the semi-permeable cell membrane.

1.1.4 Reduction to Two Dimensions

The HH model is a four-dimensional system: three gating variables m, h, n and the membrane potential V. To analytically describe the dynamics of a conductance-based

neuron model it is beneficial to reduce the number of degrees of freedom; specifically use a *quasi-steady state approximation.*

The general approach is with *separation of time scales* where the dynamics of fast gating variables - small values of τ_m - compared to slow gating variables - large values of $\tau_{h,n}$ - effectively allows the Na^+ activation current to be treated as instantaneous. That is, changes in $m(t)$ are immediately accounted for as changes to $V(t)$. The sodium activation gating variable is no longer a degree of freedom for the system; it is replaced with its steady state value $m(t) \to m_\infty(V)$.

Since $\tau_h(V), \tau_n(V)$ have mirrored dynamics and $n_\infty(V), 1-h_\infty(V)$ are nearly equivalent one can approximate the two gating variables n and $1-h$ by the single *recovery variable* w. Approximating $1 - h \approx n$ sets

$$h = 1 - w \qquad n = w \qquad m = m_\infty(V) \tag{1.11}$$

which gives the reduced 2D HH equations

$$\begin{aligned} C\dot{V}(t) &= -g_{Na} m_\infty^3(V)[1 - w(t)][V(t) - \bar{V}_{Na}] - g_K w^4[V(t) - \bar{V}_K] - g_L[V(t) - \bar{V}_L] + I(t) \\ \tau_w \dot{w}(t) &= w_\infty(V) - w(t) \end{aligned} \tag{1.12}$$

1.2 Topology of Spike Generation

When modeling channels, currents, and voltages the aim is to develop a description of or constraints on the free parameters. Qualitatively there are *only four* types of firing behaviour all neuron models can be categorized into. The elementary processes underlying how a neuron turns an input into an output are universal. Some of these fundamental properties are not obvious from the biophysical description, but can be better understood mathematically using *phase space topology.*

Without understanding universal scaling laws one would think it possible, with so many free parameters, to tune them such that any arbitrary (*e.g.* linear) $f - I$ curve could be produced. However, geometric phase space analysis allows for a proof that only two types of behaviour exists and any computational search for others would be fruitless. These robust behaviours mean a new model of such a complex system as neuronal

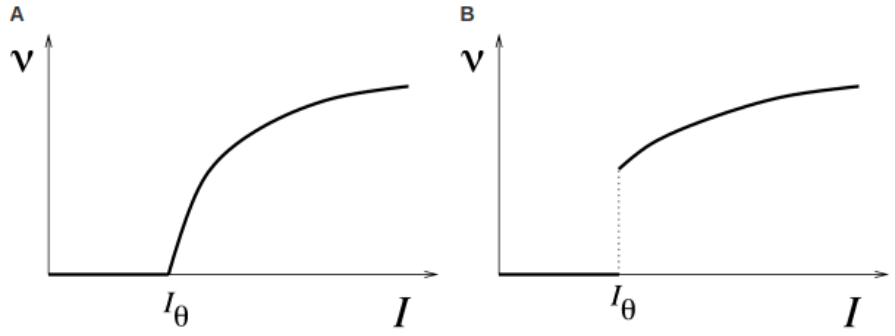

Figure 1.5: $f - I$ curve of a Type I model **(A)** and a Type II model **(B)**. I_θ is the *rheobase current*. ν is usually used to denote the firing rate instead of f. Taken from "Neuronal Dynamics" by W. Gerstner, W.M. Kistler, R. Naud, and L. Paninski [3]

populations must first satisfy phase space behaviour that is of the right kind. To make this choice an understanding of dynamic systems that are governed by topology is needed.

Phase Space Objects in 2D

Phase plane analysis is the formal tool for analyzing two-dimensional dynamical systems and exploring feasibility of different models; for example, excitability types in neurons. Using experimental data from current injected neurons the firing rate as a function of input current can be measured. The result is an $f - I$ curve, as shown in Fig 1.5. *Type I* has a continuous $f - I$ curve and *Type II* has a discontinuous $f - I$ curve. Excitatory pyramidal neurons are an example of Type I and inhibitory cortical neurons an example of Type II. How these two distinct regimes of behaviour arise can be entirely understood by discussing the dynamics using phase portraits.

The benefit of reducing the 4D HH system to 2D is it can be visually represented in phase space and action potentials can be described using *invariant sets* and *bifurcation theory*. The analysis of trajectories of $V(t)$ in the $Vt-$plane can equivalently be considered using geometric descriptions in the $Vw-$plane. Two degrees of freedom is the minimum required for a system to display oscillatory behaviour; in this case to represent a neuron's membrane potential cycling as it fires APs.

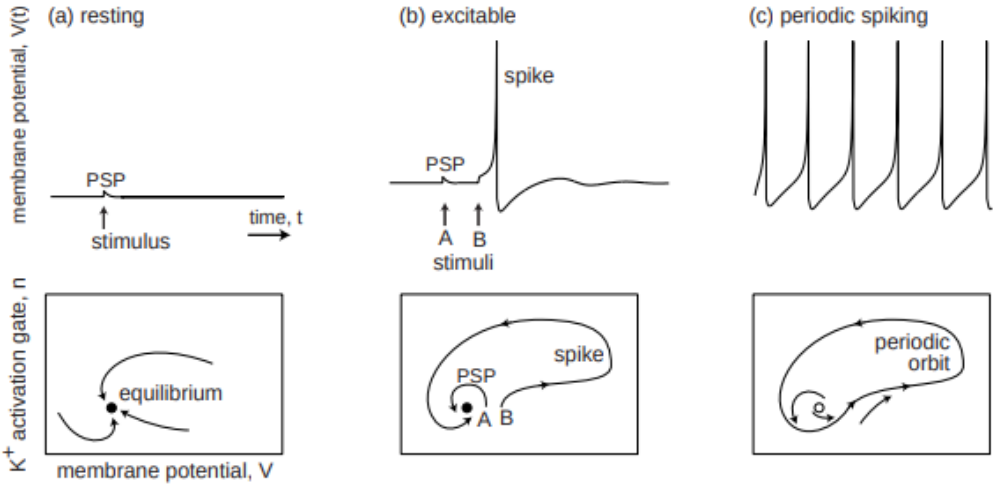

Figure 1.9: Resting, excitable, and periodic spiking activity correspond to a stable equilibrium (a and b) or limit cycle (c), respectively.

Figure 1.6: Taken from "Dynamical Systems in Neuroscience" by E. M. Itzhikevich [1]

Poincaré-Bendixon Theorem

In two-dimensional phase space the long-term behaviour of trajectories of continuous dynamical systems is completely described by *Poincaré-Bendixon theorem*. For any real differentiable function any non-empty compact subset of points is either a

- fixed point
- periodic orbit
- homoclinic/heteroclinic connected set

The fact that a spike is unitary in size constrains the amplitude of the limit cycle to be fixed. In combination with this theorem this means there are only four possible types of bifurcation a real neuron can undergo. The transition from panels (b) to (c) in Fig 1.6 is a bifurcation; the neuron transitions from a state of equilibrium to periodic firing.

1.2.1 Invariant Sets

Invariant sets are collections of points in phase space that are closed under the dynamics - beginning with any subset they will always remain on this set. The types of invariant sets in 2D are *fixed points*, *periodic orbits*, and *homoclinic orbits*.

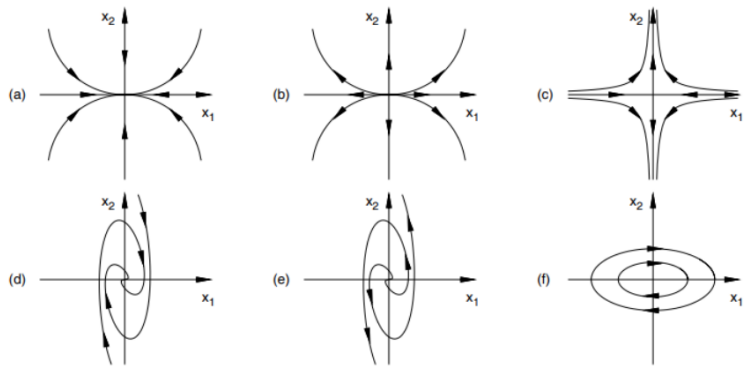

(a) **stable node** $\lambda_1 < \lambda_2 < 0$

(b) **unstable node** $\lambda_1 > \lambda_2 > 0$

(c) **saddle point** $-|\lambda_{1,2}| < 0 < \lambda_{1,2}$

(d) **stable spiral point** $\lambda_{1,2} = \mu \pm i\omega$ and $\mu < 0$

(e) **unstable spiral point** $\lambda_{1,2} = \mu \pm i\omega$ and $\mu > 0$

(f) **elliptic fixed point** $\lambda_{1,2} = \pm i\omega$

Figure 1.7: In 2D there are six possible types of fixed points. Their stability is determined by the two eigenvalues of the linear stability matrix. The solid lines show isocurves with the arrows indicating the direction of flow. Adapted from Fig. 2.5 in "Chaos: From Simple Models to Complex Dynamics" by M. Cencini, F. Cecconi, and A. Vulpani [4]

The roots of a system (also called stationary points) define the fixed points in phase space. A fixed point can be either stable, unstable, or hyperbolic as summarized in Fig 1.7. Periodic orbits can also be stable - a *limit cycle* - or unstable - a *UPO*. A limit cycle has two defining properties: (i) a period orbit enclosing a fixed point, and (ii) a closed trajectory which neighbouring trajectories converge toward. The appearance/disappearance of the limit cycle depends on the *bifurcation parameter* with the transition occurring at the *bifurcation point*.

Stable fixed points and stable periodic orbits are called *attractors*. Anything within the locality - formally defined by the *basin of attraction* - will converge onto the attractor. Oppositely, unstable invariant sets are termed *repellers*. The boundary of the basin of attraction, termed the *separatrix*, is itself an invariant repellor set. The organization of these sets in the phase space determines the evolution of a trajectory.

Last, a homoclinic orbit starts and ends at the same fixed point, whereas a heteroclinic orbit connects two fixed points; see Fig 1.8.

Question: How can one get rid of a limit cycle in a 2D phase space? Consider a simple

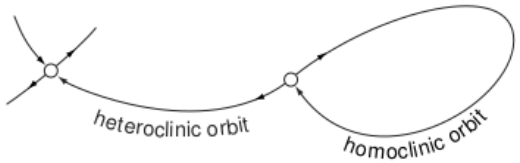

Figure 1.8: A heteroclinic orbit starts and ends at different fixed points. A homoclinic orbit starts and ends at the same fixed point, forming a closed loop. Taken from "Dynamical Systems in Neuroscience" by E. M. Itzhikevich [1]

system with a single unstable fixed point which is enclosed by a limit cycle. What transition can the system undergo to destabilize (collapse) the limit cycle?

1.2.2 Bifurcation Types

A characteristic quantity which changes value and moves a dynamical system from one qualitative behavioural regime to another is termed a *bifurcation parameter*. For the models presented here, the bifurcation parameter is the external input $I(t)$ and the bifurcation point is the *rheobase current* I_θ.

Using the terminology of phase portrait analysis, neuronal excitability is the result of a bifurcation from rest to spiking and the type of excitability is determined by the type of bifurcation. When it exists in the context of neuron firing the *limit cycle is an attractor*. Also note that the effect of a bifurcation is to *change the number and stability of fixed points*.

HOMEWORK PROBLEM: In the right-hand column of Fig 1.9 four different stable limit cycles around an unstable fixed point are shown. Move from right (spiking) to left (rest). By adding another invariant set to the locality - intermediate step in the middle column - how can the limit cycle become destabilized? Finally, once the limit cycle has collapsed what objects will the local phase space contain, left-hand column? HINTS:

- Supercritical - limit cycle originates from instability of fixed point
- Subcritical - if a limit cycle exists it is of constant amplitude
- SNIC - reduce the speed of one position on limit cycle arbitrarily low
- Homoclinic - a saddle node in the vicinity cause the orbit to become a limit cycle

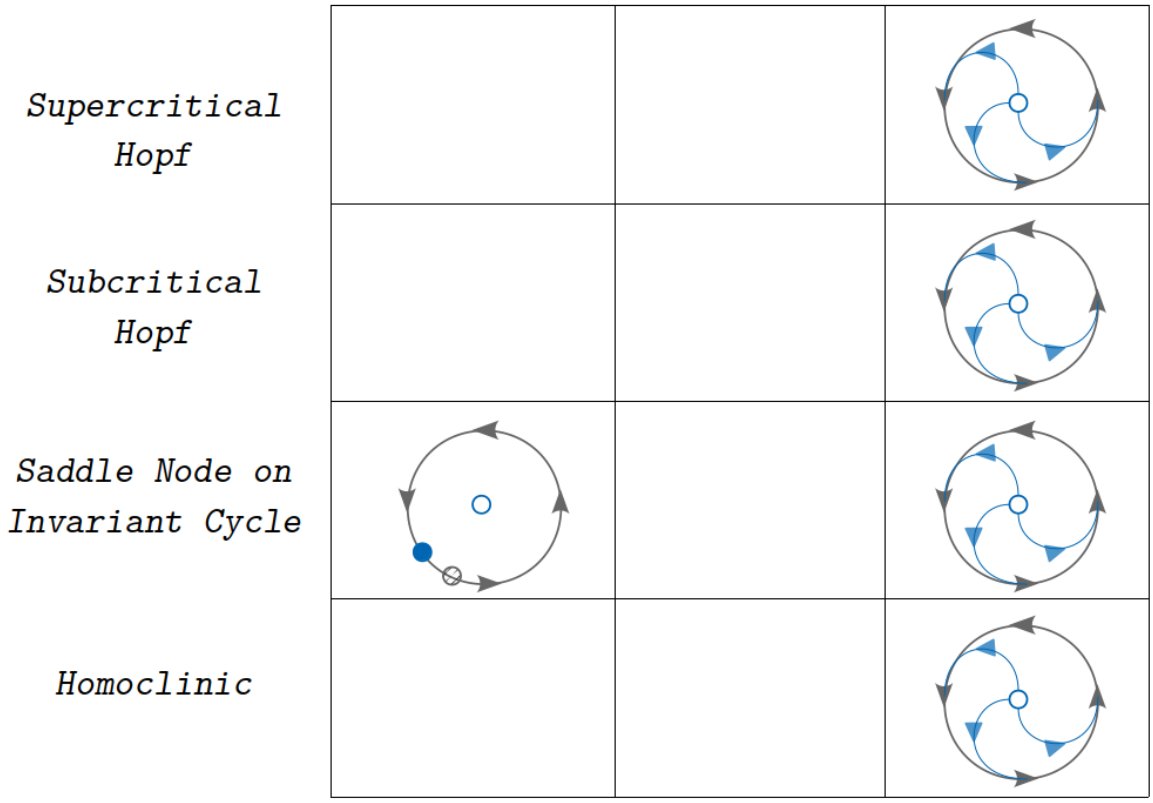

Figure 1.9: Sketch the dynamics of how the limit cycle (grey) around the unstable fixed point (blue) can lose stability and collapse. A periodically firing neuron is a closed orbit in phase space, whereas at rest the limit cycle has vanished. As an example, the equilibrium scenario for a SNIC bifurcation has been included - the solid circle is a stable node and the hatched circle is a saddle node.

Saddle Node on Invariant Circle Bifurcation

A *saddle node bifurcation* occurs when two of a system's fixed points are a *stable node* and a *saddle node*. As the bifurcation parameter is increased these two points move closer together in phase space until merging ('annihilating') at the bifurcation point. This is shown in Fig 1.10.

If a limit cycle - stable orbit around a third *unstable node* - exists in the vicinity of these two fixed points then as they annihilate (and the resting state vanishes) the trajectory converges towards the attractor. Before the point of bifurcation an invariant circle exists. At the bifurcation point this becomes a limit cycle (again enclosing the third fixed point); refer to Fig 1.11a. Once on the limit cycle the neuron fires periodic (tonic) spikes. This type of resting to firing state transition is a *saddle node on invariant circle*

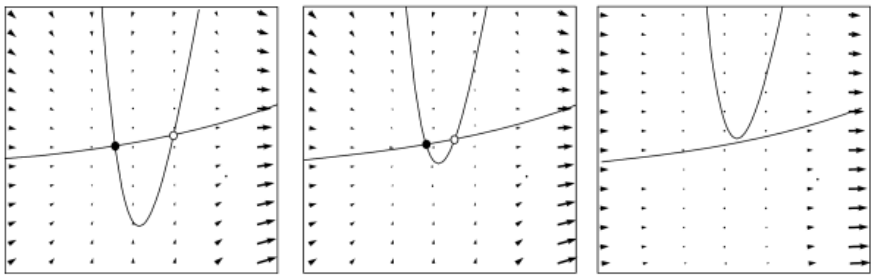

Fig. 4.12: Saddle-Node Bifurcation. The u-nullcline is represented as a parabola that moves upward as the current is increased (from left to right). The saddle point is shown as an open circle and the node as a filled circle. When the current is increased, the two fixed points, which are initially far apart (left,) move closer together (middle) and finally annihilate (right).

Figure 1.10: Taken from "Neuronal Dynamics" by W. Gerstner, W.M. Kistler, R. Naud, and L. Paninski [3]

(SNIC) bifurcation.

Subcritical Hopf Bifurcation

Also commonly referred to as *Andronov-Hopf bifurcations*, this type of bifurcation is characterized by loss of stability of fixed points with concurrent emergence of an oscillation. This occurs in systems where the fixed points are spiral points, namely the eigenvalues are complex $\lambda_{\pm} = \mu \pm i\omega$. If the real part is negative, $\mu < 0$, the spiral point is stable or if positive, $\mu > 0$, then unstable.

As the bifurcation parameter increases the real part of the eigenvalue changes from negative to positive, resulting in spiral points losing stability; now $\lambda_{\pm} = \mu \pm i\omega$ where $\mu > 0$. Whereas before there were oscillations of zero amplitude, now there are oscillations of increasing amplitude. For a *subcritical Hopf bifurcation* the oscillation is unstable close to the bifurcation point. For a *supercritical Hopf bifurcation* the oscillation is always stable. This is described in Fig 1.12.

To reiterate the difference, for a subcritical Hopf bifurcation the limit cycle occurs before the loss of fixed point stability. In contrast, for a supercritical Hopf bifurcation the limit cycle only emerges after the fixed point has lost stability. This difference is depicted in Fig 1.11b,c. *Neurons do not undergo supercritical Hopf bifurcations because action potentials are unitary in size.*

For completeness it must be mentioned that for a subcritical Hopf bifurcation the $f - I$

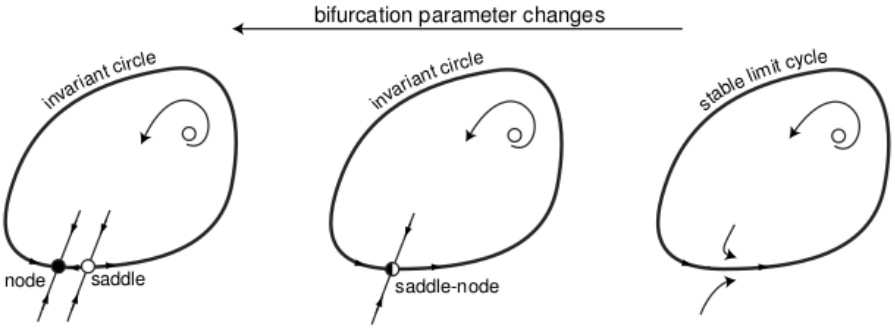

(a) Saddle node on invariant circle bifurcation

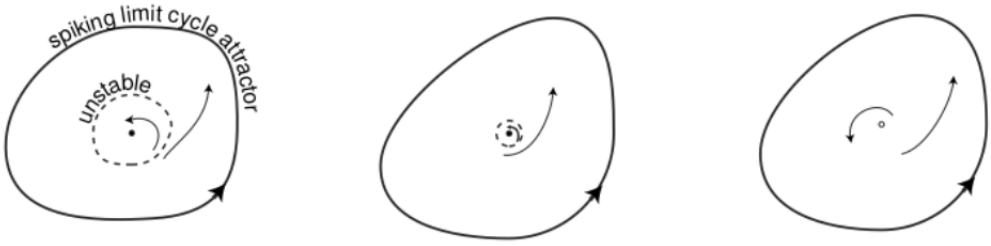

(b) Subcritical Hopf bifurcation

(c) Supercritical Hopf bifurcation

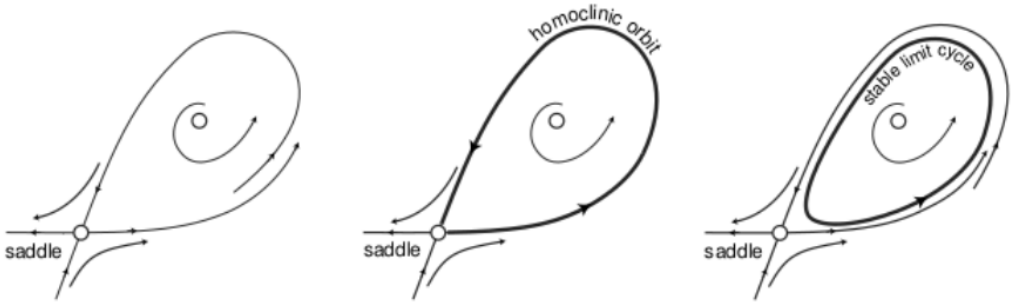

(d) Homoclinic orbit bifurcation

Figure 1.11: The four possible types of bifurcation a real neuron can undergo to transition from rest (left column) through the bifurcation point (middle column) to a stable spiking state of fixed oscillations on a limit cycle. Adapted from "Dynamical Systems in Neuroscience" by E. M. Itzhikevich [1]

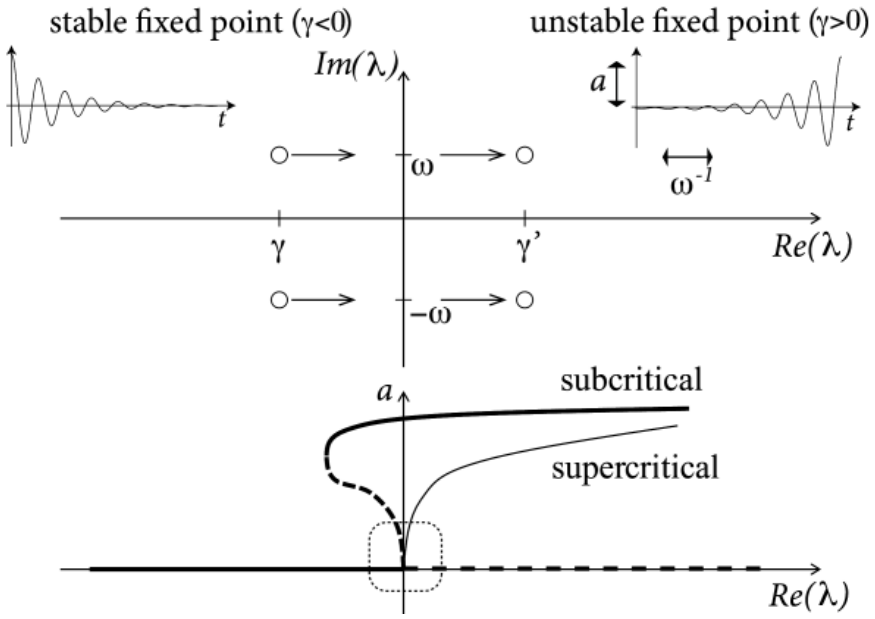

Figure 1.12: The difference between a subcritical and supercritical Hopf bifurcation is a result of the real part of the eigenvalues of the linear stability matrix becoming positive. γ is equivalent to μ as defined as the real part of eigenvalues used in these notes. Taken from "Neuronal Dynamics" by W. Gerstner, W.M. Kistler, R. Naud, and L. Paninski [3]

curve displays hysteresis around the bifurcation point (not shown). This is because the limit cycle exists before the bifurcation point as $I(t) \rightarrow I_\theta^-$ (alternatively, does not disappear at the bifurcation point if decreasing from $I(t) \rightarrow I_\theta^+$) so stable large amplitude trajectories - spikes - remain possible in a region of bi-stability around I_θ.

Homoclinic Orbit Bifurcation

This type of bifurcation is often described as a limit cycle colliding with a saddle node, as shown in Fig 1.11d. Before bifurcation a stable limit cycle exists (around a second unstable fixed point) in the vicinity of a saddle node. As the bifurcation parameter is increased the limit cycle expands until the saddle point lies on it - at this point the cyclical trajectory is a homoclinic orbit. If the input continues to increase the locality becomes unstable; an additional diagram depicting this is the contents of Fig 1.13.

1.2.3 Firing Onset

Periodic spiking corresponds to a limit-cycle in the $Vw-$plane in phase space. The transition from rest to spiking is geometrically equivalent to a trajectory transitioning

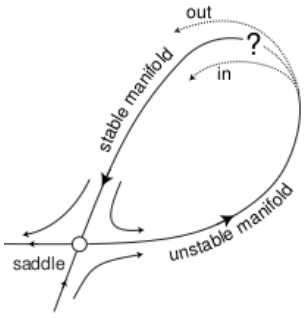

Figure 6.27: Saddle homoclinic orbit bifurcation occurs when the stable and unstable submanifolds of the saddle make a loop.

Figure 1.13: Taken from "Dynamical Systems in Neuroscience" by E. M. Itzhikevich [1]

from movements about the fixed points to movement on a stable periodic orbit. The threshold for neuronal firing, as well as excitability types, can be described using the concepts of *nullclines* and *flow patterns* in phase space.

This discussion will use the *persistent sodium plus potassium* $I_{Na,p} + I_k$ model (which uses equivalent equations to describe the dynamics as the *Morris-Lecar model*).

Nullclines

A *nullcline* is a special case of an isocurve - all points along it have the same value - but they specifically represent trajectories in phase space where one degree of freedom is stationary. Here phase space is the collection of all points $\{(V, w)\}$ and the flow pattern (vector field) at each point is given by $(\dot{V}, \dot{w})$; as shown in Fig 1.14A. Note that the size of each arrow is proportional to the magnitude of $(\dot{V}, \dot{w})$ at that point.

The V-nullcline is the set of all points where $\dot{V} = 0$ and the w-nullcline is the set of all points where $\dot{w} = 0$. Along the V-nullcline ($\dot{V} = 0, \dot{w} \neq 0$) the direction of flow, indicated by arrows, can only be perpendicular (vertical in this case). Likewise, along the w-nullcline ($\dot{V} \neq 0, \dot{w} = 0$) the flow can only be in perpendicular directions (horizontal in this case). This is depicted in Fig 1.14B. Note that when moving along a nullcline the direction of arrows will flip after passing through a fixed point.

The *intersection points* ($\dot{V} = 0, \dot{w} = 0$) of the two nullclines are the *fixed points*. Therefore with phase portrait analysis the number and type of fixed points can be found. Nullclines can be used to determine the stability of fixed points, in place of eigenvalue analysis, to determine the direction of the flow pattern.

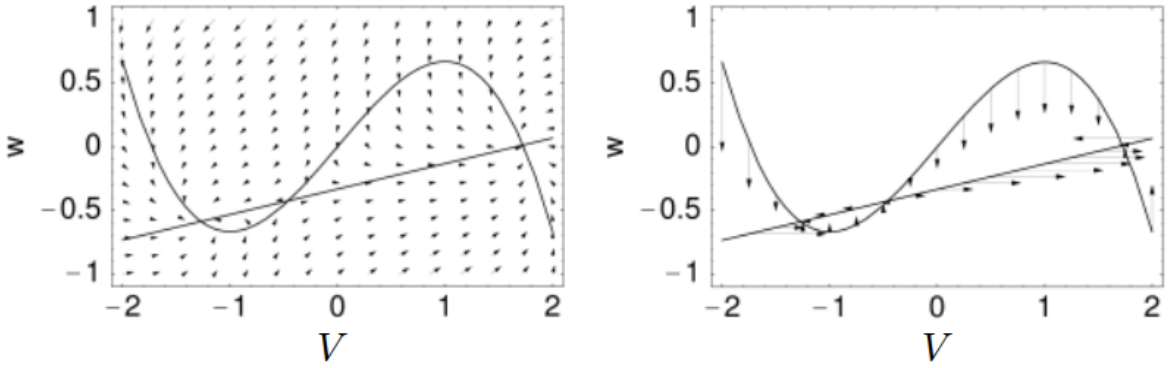

Figure 1.14: (left) A phase portrait displaying the vector field for a 2D HH-like model. **(right)** Only the nullclines are shown with flow arrows with a flip of direction at each intersection point. Adapted from "Neuronal Dynamics" by W. Gerstner, W.M. Kistler, R. Naud, and L. Paninski [3]

Morris-Lecar Model

A conductance-based model qualitatively similar to the reduced HH system is the Morris-Lecar model which describes excitability using a slow hyperpolarizing K^+ current and an instantaneous Ca^{2+} current. Originally it was developed to explain muscular activity (using experimental data from barnacles). Using the same form of the equations, but replacing Ca^{2+} with Na^+ gives the *persistent sodium plus potassium model*.

$$C\dot{V} = g_L[\bar{V}_L - V] + g_{Na}m_\infty(V)[\bar{V}_{Na} - V] + g_K w(t)[\bar{V}_K - V]$$
$$\tau(V)\dot{w}(t) = w_\infty(V) - w(t)$$

The $w-$nullcline is given by the equation $w_\infty - w = 0$ where the form of w_∞ is as specified in the model

$$w = w_\infty = \frac{1}{2}\left[1 + \tanh\left(\frac{V - u_1}{u_2}\right)\right] \tag{1.14}$$

with u_1, u_2 being tunable parameters. The $V-$nullcline is given by the equation $\dot{V}(t) = 0$ which has the solution of a cubic parabola given by

$$w = \frac{I_{ext} + g_L(\bar{V}_L - V) + g_{Na}m_\infty(\bar{V}_{Na} - V)}{g_K(\bar{V}_K - V)} \tag{1.15}$$

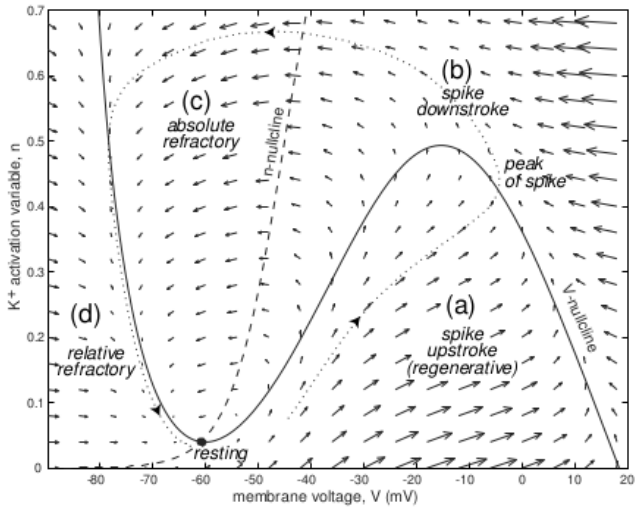

Figure 1.15: The $V-$nullcline and $w-$ nullcline for the Morris-Lecar model with parameters adjusted to exhibit Type I firing onset. The flow pattern (vector field) is shown and relates the regions in phase space to action potential generation. Taken from "Dynamical Systems in Neuroscience" by E. M. Itzhikevich [1]

A representation of the phase plane into the four quadrants given by the set $\{\pm\dot{V}, \pm\dot{w}\}$ with two nullclines and flow pattern (vector field) as shown in Fig 1.15. The two nullclines have one intersection point which is, by definition, a fixed point since being on both nullclines requires $(\dot{V} = 0, \dot{w} = 0)$. There will always be an odd number of intersections (with one being the minimum) in such a system as a result of distorting in a continuous fashion two continuous curves. As the bifurcation parameters I_{ext} changes the position of the V-nullcline will shift causing the location of the intersection point to move.

Subcritical Hopf Bifurcation Dynamics

For a different choice of free parameters u_1, u_2 this same system undergoes a subcritical Hopf bifurcation and exhibits Type II dynamics. The phase portrait for this scenario is the contents of Fig 1.16(left). In this system there is no separatrix and so in the long-term beginning from any initial point the trajectory will return to the single fixed point.

A positive perturbation from rest will cause a trajectory to evolve from a position in the vicinity of the fixed point; however, due to the direction of the flow field there is no direct return path. Instead they must go 'up and around' in a counter-clockwise direction. The larger the perturbation, the longer the return path, and therefore the

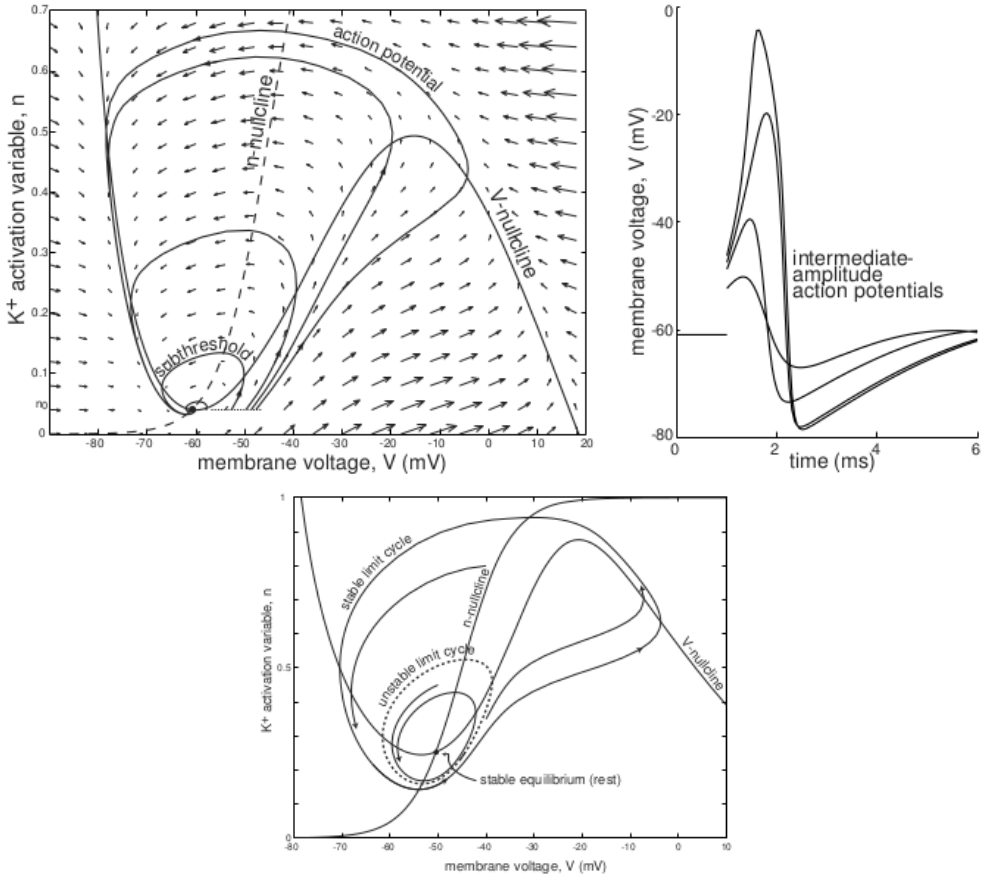

Figure 1.16: (left) Phase portrait for a system having undergone a subcritical Hopf bifurcation. Different magnitude perturbations from the fixed point cause increasing large detours on a counter-clockwise return path. **(right)** Amplitude of corresponding 'spike-like' events. **(bottom)** Before bifurcation $I < I_\theta$ a stable limit cycle exists but so does a UPO (the dashed line is labeled incorrectly). The K^+ activation variable n corresponds to $w(t)$ as used in these notes. Adapted from "Dynamical Systems in Neuroscience" by E. M. Itzhikevich [1]

greater the spike.

For a single voltage excursion from threshold this gives a continuum of peak potential values. The scenario is not for repetitive firing or real action potentials, but below threshold this type of bifurcation manifests graded intermediate-amplitude 'spike-like' events as shown in Fig 1.16(right).

Question: How does this system give rise to repetitive firing?

Before bifurcation, but as I increases, the $V-$nullcline moves upwards. The fixed point

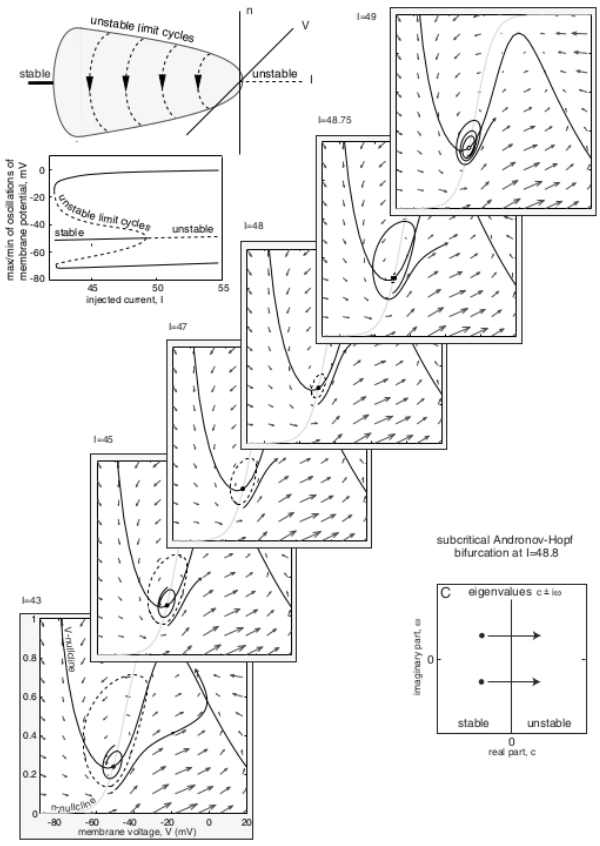

Figure 1.17: Subcritical Hopf bifurcation. For small values of the input I an unstable periodic orbit (UPO) exists - the limit cycle in the top left is incorrect. As the input I is increased this UPO shrinks until merging with the fixed point. This causes the fixed point to lose its stability and a stable limit cycle to form around it. Taken from "Dynamical Systems in Neuroscience" by E. M. Itzhikevich [1]

is shifted (as the intersection point is changing) and a UPO exists around the hyperbolic point; see Fig 1.16(bottom). To better visualize this, a three-dimensional representation is shown in Fig 1.17 with cross-sectional phase portraits. At low values of the external driving current the system is stable. As I increases a region of bi-stability occurs where there is both a fixed point (at the resting potential) and a UPO around it. As I is further increased the UPO shrinks in size until it collapses onto the fixed point - the moment this occurs the hyperbolic point becomes an unstable fixed point.

After bifurcation, if $I > I_\theta$ is held constant, the system will undergo fixed oscillations on a limit cycle which corresponds to periodic firing. The phase portrait describing this scenario (left) and the membrane voltage as a function of time (right) are shown

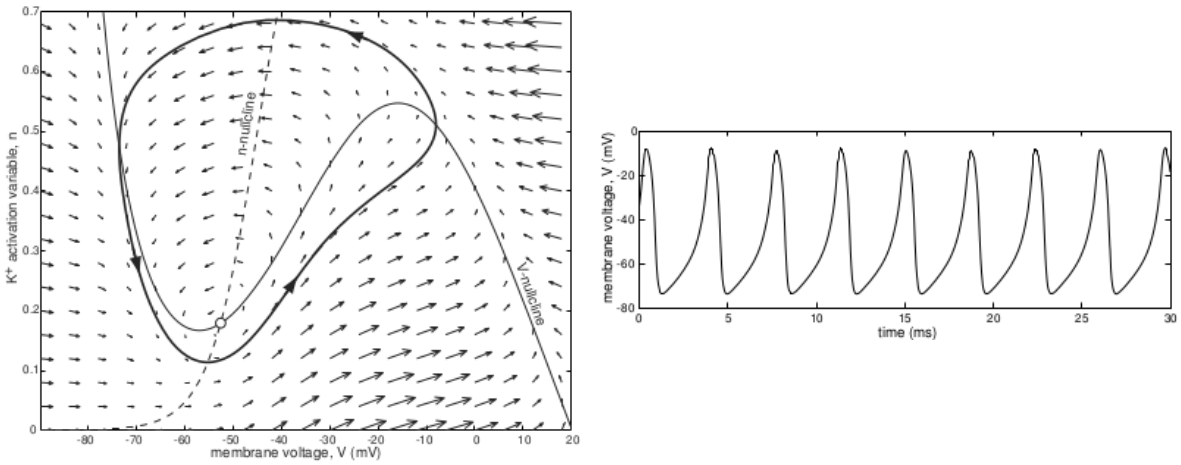

Figure 1.18: (left) Spiking as periodic oscillations on a fixed limit cycle for the subcritical Hopf bifurcation and **(right)** associated spike train. Taken from "Dynamical Systems in Neuroscience" by E. M. Itzhikevich [1]

in Fig 1.18.

SNIC Bifurcation Dynamics

Adjusting the free parameters u_1, u_2 so that the system is capable of undergoing a saddle node on invariant circle bifurcation graphically corresponds to shifting the $w-$nullcline upward. The system will now have three fixed points; this scenario is shown in Fig 1.19.

Before bifurcation, $I < I_\theta$, three fixed points exist and spiking is not possible. At the bifurcation point $I = I_\theta$ a limit cycle emerges with zero frequency. At this value flow arrows in the annihilation region are exactly zero and trajectories cannot pass through. After the bifurcation, $I > I_\theta$, all trajectories must still pass through the locality in phase space where the two previous fixed points annihilated.

Now in this region the magnitude of flow arrows is near zero and the trajectory evolves very slowly; giving rise to arbitrarily low firing frequencies. (This slow region is often called the *'ruins' or 'ghost' of the fixed points.*) As the current is increased further, the magnitude of flow in the *'ruins'* monotonically increases with the frequency of limit cycles increasing in-step. This explains the smooth onset of firing.

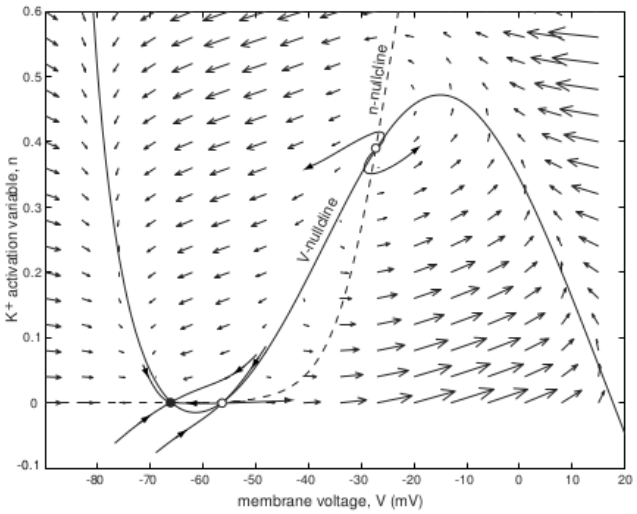

Figure 1.19: Morris-Lecar model neuron with free parameters u_1, u_2 chosen such that the system has three fixed points and can undergo a SNIC bifurcation. The K^+ activation variable n corresponds to $w(t)$ as used in these notes. Taken from "Dynamical Systems in Neuroscience" by E. M. Itzhikevich [1]

1.2.4 Excitability Types

Question: How many ways do real neurons transition from rest to repetitive firing?

A periodically spiking neuron will be undergoing oscillations on a fixed limit cycle in phase space. However, firing onset depends on the type of bifurcation. There are two main classes of neuron (models), designated *Type I* and *Type II*.

Type I Models

The smooth onset, or lack of jump discontinuity in the $f - I$ curve, is explained for Type I models as being a result of trajectories moving arbitrarily slowly through the 'ruins' of the fixed points after bifurcation.

The excitability of a Type I neuron can be explained in phase space by the role of the *stable manifold* - the isocline between the saddle node and unstable node (defined before bifurcation). A small perturbation to a trajectory near the stable manifold will return to the fixed point in one of two ways, either directly or via a detour. The former corresponds to a subthreshold change to the membrane potential, whereas the latter corresponds to a single spike.

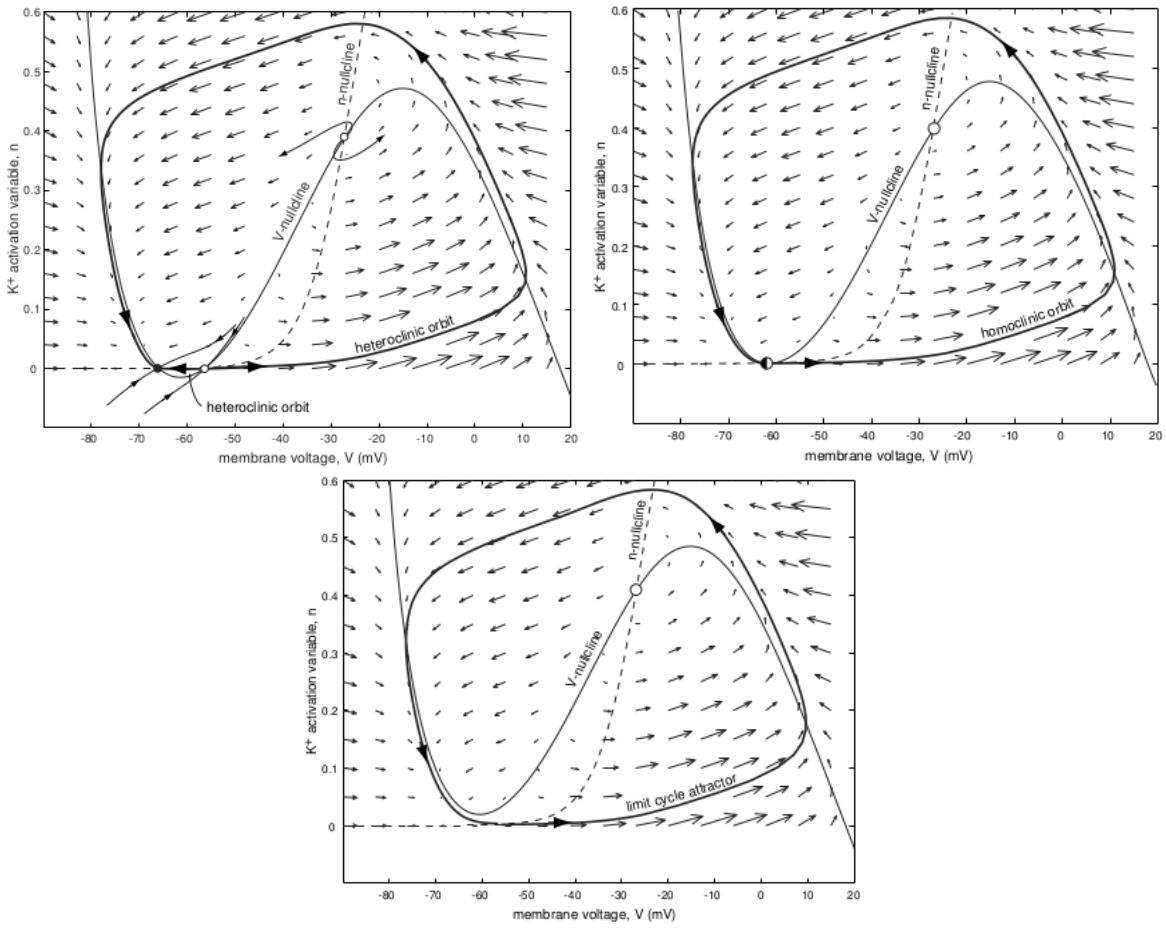

Figure 1.20: (left) Before bifurcation $I < I_\theta$ there are two heteroclinic orbits which connect the stable node and saddle node. **(right)** At the bifurcation point $I = I_\theta$ these orbits transition into a single stable homoclinic orbit. The 'ruins or ghost' of the fixed point is clearly shown as an annihilating point (black/white semicircles). **(bottom)** After bifurcation $I > I_\theta$ a stable limit cycle exists. Adapted from "Dynamical Systems in Neuroscience" by E. M. Itzhikevich [1]

The *theorem of existence and uniqueness* for ODEs means trajectories cannot intersect. Consider a point along the stable manifold and a subsequent input pulse of magnitude $\varepsilon \ll 1$ which perturbs the point a short distance to the left ($-\varepsilon \to V(t)$ decreases) or the right ($+\varepsilon \to V(t)$ increases). A shift to the left from the stable manifold will cause the subsequent trajectory to return directly to the stable node. However, a shift to the right off the stable manifold causes the subsequent trajectory to make a long circuitous excursion to return to the stable node. This is a single spike in a Type I neuron and the stable manifold is equivalent to a (geometrical) firing threshold. This is depicted in Fig 1.21.

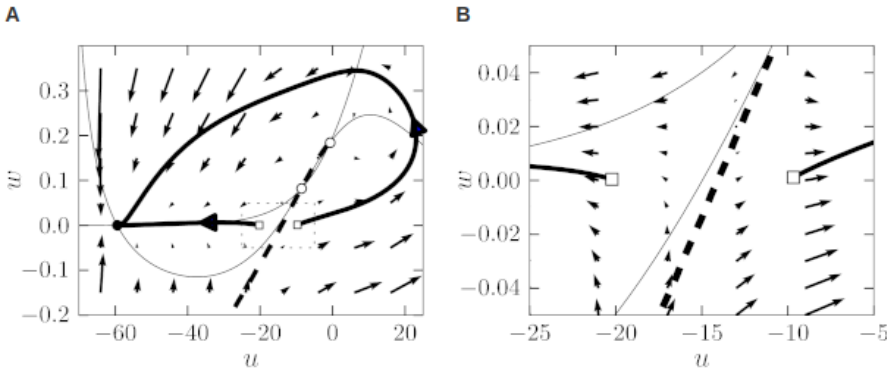

Fig. 4.17: Threshold in a type I model. **A**. The stable manifold (thick dashed line) acts as a threshold. Trajectories (thick solid lines) that start to the right of the stable manifold cannot return directly to the stable fixed point (filled circle) but have to take a detour around the repulsive fixed point (circle at $(u, w) \approx (-1, 0.2)$). The result is a spike-like excursion of the u-variable. Thin lines are the nullclines. **B**. Blow-up of the rectangular region in A. The starting points of the two sample trajectories are marked by squares.

Figure 1.21: Here u corresponds to V as used in these notes for the membrane potential. Taken from "Neuronal Dynamics" by W. Gerstner, W.M. Kistler, R. Naud, and L. Paninski [3]

Type II Models

A Hopf bifurcation occurs when a limit cycle emerges due to the loss of stability of a system's fixed points. For subcritical Hopf bifurcations this limit cycle comes into existence at the bifurcation point with a non-zero frequency. This is because oscillations only emerge when the fixed point loses its stability - transitions from a stable node to an unstable node - and at this point they have large *finite* amplitude. This large amplitude corresponds to a non-zero frequency and the frequency of a limit cycle is the firing rate; hence the jump discontinuity in the $f - I$ curve.

Said differently, the limit cycle only exists for a finite frequency - trajectories cannot traverse a large amplitude loop at arbitrarily low frequencies - and this is what creates the jump discontinuity in the $f - I$ curve. As the bifurcation parameter $I(t)$ increases past the bifurcation point I_θ the neuron transitions from rest to finite frequency periodic firing. If $I > I_\theta$ continues to increase, the amplitude and therefore frequency of the limit cycle both monotonically increase as well, which explains the continuing increase in firing rate.

For Type II models there is no analogous stable manifold which acts as a threshold. The closest thing to an effective threshold in Type II models is the *middle branch of the* $V-$*nullcline*. This is the section between one minimum and one maximum as displayed

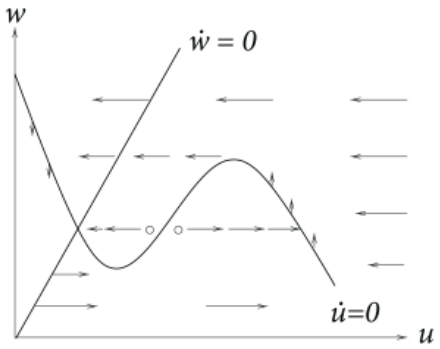

Fig. 4.21: Excitability in a type II model with separated time scales. The u-dynamics are much faster than the w-dynamics. The flux is therefore close to horizontal, except in the neighborhood of the u-nullcline (schematic figure). Initial conditions (circle) to the left of the middle branch of the u-nullcline return directly to the stable fixed point; a trajectory starting to the right of the middle branch develops a voltage pulse.

Figure 1.22: Here $\dot{u}$ corresponds to $\dot{V}$ as used in these notes for membrane potential. Taken from "Neuronal Dynamics" by W. Gerstner, W.M. Kistler, R. Naud, and L. Paninski [3]

in Fig 1.22.

HOMEWORK PROBLEM: What is Type III excitability called, how are firing rate and input current related, and why is this not a main category of neuron classification? HINT: It was identified by Hodgkin and Huxley and corresponds to a single 'one-off-event' spike.

1.3 Universal Shapes of $f - I$ Curves

One definition of firing rate of a *single* neuron is the inverse of the average time between spikes - termed *interspike interval (ISI)* - which is equivalent to the period of oscillation in phase space. Since the rate of spiking is dependent on the external current the ISI period is as well, $T_{isi}(I_{ext})$. The calculation of this period is dependent upon the type of bifurcation which produces the limit cycle.

Firing Rate Saturation

Due to the finite time duration of an action potential there is an upper bound on firing rate at which the $f - I$ curve saturates (not shown). In addition there is a post-spike hyperpolarization when firing is not possible. Assuming the AP and refractory period occur with a combined duration of 1 $[ms]$ this gives $\nu_{max} \approx 1$ $[kHz]$; an order of magnitude approximation.

1.3.1 Saddle Node on Invariant Cycle

First consider the case of a SNIC bifurcation. In the 'ghost or ruins' of the fixed points, near the bifurcation point at the onset of spiking, the voltage dynamics are described by

$$\dot{V}(t) = V^2(t) + I_{ext}(t) \tag{1.16}$$

and the corresponding period of firing where V_T is the *threshold voltage* at which a 'point-of-no-return' spike fires

$$T_{isi} = \int_{-V_T}^{V_T} dt = \int_{-V_T}^{V_T} dV \frac{1}{V^2 + I} = 2\int_0^{V_T} dV \frac{1}{V^2 + I} = \frac{2}{\sqrt{I}} \arctan(\frac{V_T}{\sqrt{I}}) \tag{1.17}$$

The arctan term asymptotes and in the $\lim V_T \to \infty$ this reduces to $(I_{ext} - I_0)^{-1/2}$. Therefore, one can express the firing rate of a SNIC neuron (with $I_0 = 0$) as

$$\nu_{SNIC}(t) = \frac{1}{T_{isi}(I_{ext})} \sim \frac{1}{\sqrt{I_{ext}}} \tag{1.18}$$

If $I_{ext} = 0$ then $\dot{V} = V^2$. It is known that if on the RHS the term is not squared (*i.e.* to the power of one) then $lim\ V(t \to \infty) \to \infty$. That is, the function will go to infinity over an infinite amount of time. Conversely for $\dot{V} = V^2$ *finite time blowup* occurs, namely $V(t) \to \infty$ but in a finite amount of time. This class of ODEs do not have solutions for all times.

HOMEWORK PROBLEM: Consider the general case of $\dot{V} = V^\beta$. Which of the two behaviours, standard exponential divergence or finite time blowup is expected? Are there particular values of β that give finite time blow up or is $\beta = 2$ a special case? HINT: $\int_0^T dt = \int_0^\infty dV\ V^{-\beta}$

The Normal Form

Taking the threshold as going to infinity and imposing periodic boundary conditions $\lim V_T \to \infty = \lim V_T \to -\infty$ lets an equivalent phase representation be used. Letting θ be the trajectory angle on the limit cycle (defined relative to some arbitrary point chosen as $\theta = 0$) then the change of variables $V = \tan(\theta/2)$ in the equation $\dot{V} = V^2 + I$ gives

$$\dot{\theta} = (1 - cos\theta) + I(1 + \cos\theta) \tag{1.19}$$

As in other areas of physics, the framing of a problem heavily depends on the choice of representation. For SNIC bifurcations the simplest framework, in general defined as the *normal form*, is the phase representation. (This specific example is usually referred to as the *theta neuron model*.)

1.3.2 Homoclinic Orbits

Now consider the case of a homoclinic bifurcation. A hyperbolic fixed point has a stable and an unstable manifold which are not necessarily orthogonal. The directions are dependent upon the eigenvalues $\lambda_{1,2}$ of the *linear stability matrix* and are aligned with the corresponding eigenvectors $\mathbf{e_{1,2}}$. In the vicinity of the fixed point to first-order

$$\mathbf{x}(t) = a_1\mathbf{e}_1^{-\lambda_1 t} + a_2\mathbf{e}_2^{-\lambda_2 t} \tag{1.20}$$

Question: How long will this dynamic system spend in the vicinity of the collision point just after bifurcation (where the limit cycle is local to the hyperbolic fixed point)?

For a homoclinic bifurcation the hyperbolic point and limit cycle collide. The position at which a trajectory exits the limit cycle and enters the vicinity of the hyperbolic point is primarily dependent on distance between the two objects. Going from large to small values of I the approach becomes closer and the frequency slower in that region. ISI period is the duration that the trajectory is in the vicinity of the hyperbolic fixed point. This only depends on the unstable manifold; therefore ignore second eigenvector term. Letting $\tau_1 = -\lambda_1^{-1}$ and knowing $a_1 \sim I_{ext}$ the firing rate is approximately given by

$$V_T \sim a_1 e^{t/\tau_1} \tag{1.21a}$$

$$\therefore \ln\left(\frac{V_T}{a_1}\right) \approx \frac{T}{\tau_1} \tag{1.21b}$$

$$\nu_{homo} \approx \frac{1}{\tau_1 \ln(V_T/a_1)} \tag{1.21c}$$

$$\therefore \nu_{homo} \approx \frac{1}{\tau_1 \ln(I_{ext}/a_1)} \tag{1.21d}$$

Description of homoclinic bifurcation requires treatment with two degrees of freedom and so no one-dimensional normal form exists.

1.3.3 Adaptive Spiking

By observing spike train patters from experimental data it is found that real neurons are not perfect periodic oscillators and instead can exhibit a time-dependent interspike

interval. (There are numerous types of neuronal firing patterns.) Spikes later in a spike train have larger ISI due to a phenomenon called *firing rate adaptation* which results in an approximately linear $f-I$ curve.

A current source, such as specific ion channels in the system, make it more difficult for the neuron to fire as they allow positive ions to leave the cell in increasing number as the external current - and membrane voltage - is increased. In turn, this causes delays in spiking, resulting in increasing ISI, until a biophysically constrained maximum is obtained. For greater values of input current (and membrane voltage) the lipid bilayer becomes unstable and deteriorates.

This adaptation current is firing rate dependent and denoted $I_{adap}(\nu)$. Biophysically after each AP Ca^{2+} enters the cell and voltage-dependent calcium ion channels play the role of facilitating the additional adaptation current. Calcium is a proxy for firing rate - the higher the firing rate the greater the concentration of calcium - that moves the potential farther away from the voltage threshold.

The firing rate is now not only a function of I_{ext} but the current that is effectively driving the spiking, such that $\nu_{adap} = f(I_{ext} - I_{adap}(\nu))$. Using the auxiliary variable z as a measure of the activation strength and a conversion coefficient g, the adaptation current can be written as $\nu_{adap} = f(I_{ext} - gz)$. Regardless of the effect on the $f-I$ curve the point of firing onset will not change; adaptation changes the shape of the $f-I$ curve, but not the value of I_θ.

The adaptation variable will be proportional to the rate of spiking $z = \beta f(I_{ext} - gz)$ where β is a proportionality constant. The derivative with respect to external current is given by

$$\frac{dz}{dI_{ext}} = \beta f'(I_{ext} - gz)\left[1 - g\frac{dz}{dI_{ext}}\right] \tag{1.22a}$$

$$\frac{dz}{dI_{ext}} = \frac{\beta f'(I_{ext} - gz)}{1 + \beta g f'(I_{ext} - gz)} \tag{1.22b}$$

Solving for z is non-trivial. Instead consider the behaviour of the function in the vicinity of firing onset. Near threshold the slope of the curve is divergent at onset. Therefore $f'(I_\theta - gz) \to \infty$, the $+1$ in the denominator is negligible and the result approximately

simplifies to

$$\frac{dz}{dI_{ext}} = \frac{1}{g} \qquad \longrightarrow \qquad \nu_{adap} = \frac{I_{ext}}{\beta g} \tag{1.23}$$

The only terms that have survived are the proportionality constants β, g . The adaptation current is independent of all biophysical parameters in the model. This is because of the universal property that the $f-I$ curve is arbitrarily voltage-sensitive near the point of firing onset.

$f-I$ Curve Linearization

A microscopy image of a cortical pyramidal neuron is shown in Fig 1.23A. Using patch clamping the trans-membrane voltage can be measured under an applied external current to produce a spike train; seen in Fig 1.23B for three different amplitudes of current step. Careful observation shows that the ISI is not constant, but is increasing with continued spiking.

Topographically this means there is not a single fixed frequency with which a limit cycle in phase space is traversed - evidence a real neuron is not a true two degree of freedom system - but there is another dimension represented by an *adaptation variable*. (The biological/physiological definition of adaptation is a weakening response to persistent stimulus.)

As a consequence of adaptation an empirical $f-I$ curve can be *approximately linear* - if instantaneous frequency of firing is taken to be the inverse of ISI. (Firing onset at rheobase I_θ remains.) This observation, shown in Fig 1.23C , is often taken as evidence that piecewise linear input/output relationships are what the brain primarily uses (and are the most frequently used basis for artificial neural networks).

The importance of experimental observations is to ensure models reproduce what is actually happening in real neurons and brain regions. A discussion of the vast empirical work on *in vitro* and *in vivo* neurons and the myriad models proposed to explain such findings is too extensive to be covered in these notes. Instead these (and other similar results) highlight both the descriptive strengths and quantitative gaps that simple neuron models provide.

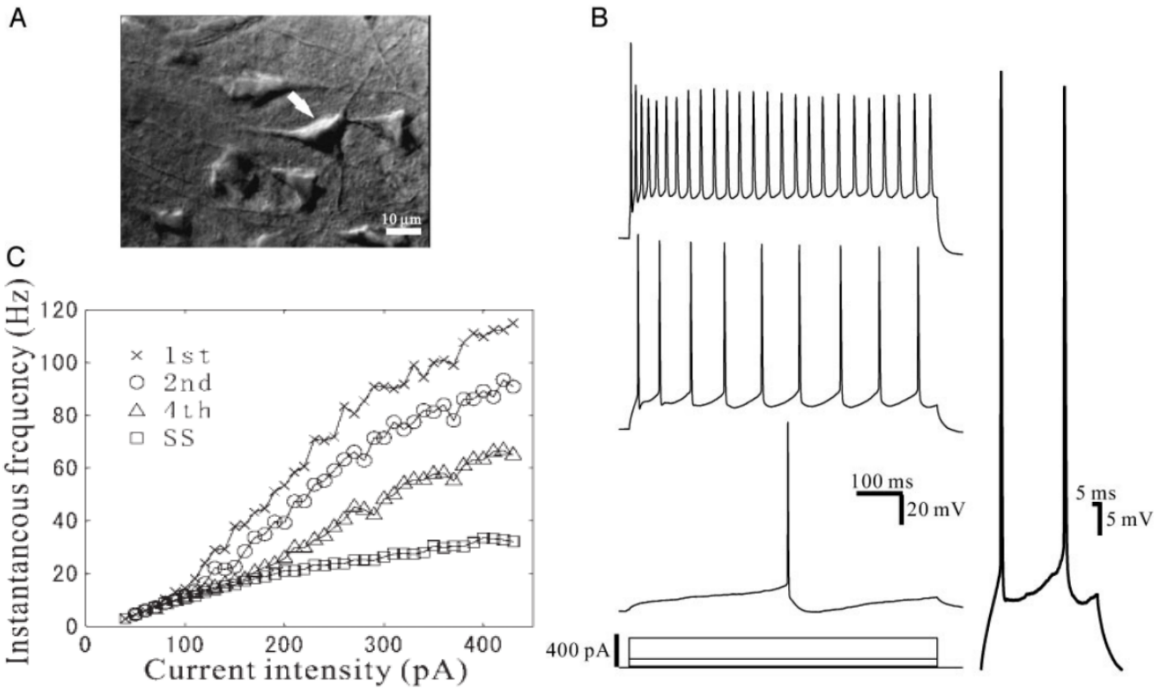

Figure 1.23: "Subthreshold and firing properties of regular spiking neurons in layer 2/3 somatosensory cortex. **(A)** Photomicrograph of a typical regular-spiking (RS) neuron, with pyramidal morphology. **(B)** Repetitive firing of RS cells for 3 different current steps of increasing amplitude... **(C)** RS neuron $f-I$ relationship. Frequencies corresponding to the 1st, 2nd, and 4th intervals and the steady-state (SS) frequency increased monotonically with the current strength, starting from 2 to 4 spikes/s, as low as could be assessed with this stimulus duration..." Caption quoted from and images adapted from Figures 1A,B and 4B in T. Tateno, A. Harsch, and H.P.C. Robinson, *J. Neurophysiol.* (2004) [5]

Chapter 2

Population Rate Dynamics

Consider a group of N neurons each engaged in the same information processing task. Their collective output is the totality of spikes that they produce and send to the rest of the brain. Each nerve cell produces its own spike train and single neurons fire sparsely. The advantage at the population level is the compound firing rate of the entire computational ensemble can be very fast. Therefore this is a quantity that can change rapidly and have a causal effect. By that reasoning the population firing rate $\nu(t)$ is a sum over the individual spike trains of the constituent neurons.

$$\nu(t) = \frac{1}{N}\sum_{i=1}^{N}\nu_i = \frac{1}{N}\sum_{i=1}^{N}\sum_{j=1}^{K}\delta(t_i^j - t) \tag{2.1}$$

where K is the total number of spikes for each neuron. The benefit is that population rate is a computationally *fast variable*. Within a large *asynchronous* population there will always be a subset of neurons that are close to threshold and can be immediately brought to spike by an external input.

The other important conceptual aspect of the dynamics of population firing rates is equations of motion are written with regard to $\dot{\nu}(t)$. The most general type of description is given by a simple approximation

$$\tau\dot{\nu(t)} = -\nu(t) + \phi(I_{input}) \tag{2.2}$$

where τ is the associated timescale of the dynamics.

2.1 Population Level Description

Description of population activity requires mapping the dynamics of single constituent neurons onto a *stochastic differential equation (SDE)*. Using the duality between SDEs and the *Fokker-Planck equation (FPE)* one can obtain a description for the evolution of the time- and voltage-dependent *probability density*.

2.1.1 Probability Density

$P(V,t) \equiv P(V(t),t)$ is a dynamical variable which describes the entire state of the system. It is a probability density which contains the probability that a single neuron at time t has membrane voltage $V(t)$. The membrane potential $V(t)$ is the state variable.

To begin, express population rates in terms of the density function. To study the dynamics of the population rates the temporal dynamics of the density $\partial_t P(V,t)$ are required. Since the total number of neurons is conserved, density must be normalized and conserved. Expressed in the form of a *continuity equation*

$$\partial_t P(V,t) = -\partial_V \psi(V,t) \tag{2.3}$$

where $\psi(V,t)$ is termed the *probability flux*. That is, time evolution of the density is the divergence of the probability flux. The normalization condition is

$$\int dV \; P(V,t) = 1 \tag{2.4}$$

2.1.2 Langevin Equation

The Langevin equation is a *stochastic differential equation (SDE)* of motion for a degree of freedom being acted upon by a deterministic - macroscopic - component and a stochastic - microscopic - component. The most general form of an SDE is given by

$$dx = a(x,t)x(t) + b(x,t)\eta(t) \tag{2.5}$$

where $a(x,t)$ is the *drift vector* and $b(x,t)$ is the *diffusion matrix*. In 1D these are scalars and simply referred to as coefficients.

The *Langevin equation* in different forms describes the two most fundamental stochastic

process in biophysics: the *Wiener process* and the *Ornstein-Uhlenbeck process*. Newton's equation for the familiar example of a Brownian particle immersed in water is

$$m\ddot{x}(t) = -\gamma\dot{x}(t) + \eta \tag{2.6}$$

where γ is the viscous drag force and η is a *random fluctuating* force representing bombardment of the Brownian particle from molecules in the liquid.

Wiener Process

The Wiener process has a vanishing drift coefficient $a(x,t) = 0$ and a constant diffusion coefficient $b(x,t) = D = 1$. (The choice $D = 1$ is for simplicity.) The Langevin equation describing the Wiener process is

$$\dot{x}(t) = \eta(t) \tag{2.7}$$

Integrating yields

$$x(t) = \int_0^t dt'\ \eta(t') \equiv W(t) \tag{2.8}$$

where $W(t)$ is the Wiener process. The mathematical details are omitted here, but technically Eqn (2.7) is inconsistent because $\eta(t)$ is not strictly differentiable and only in integral form Eqn (2.8) is it consistent. Importantly, the *Wiener increment* is rigorously defined as

$$dW(t) \equiv dW(t+dt) - dW(t) = \eta(t)dt \tag{2.9}$$

The relevance of the Wiener increment as regards neuronal signalling is it describes *Gaussian white noise*. The *noise term* η follows a Gaussian distribution with zero mean and unity variance; that is

$$\eta \sim \mathcal{N}(0,1) \tag{2.10}$$

Taking the ensemble average allows for calculation of the mean and variance (the full derivation is based on the 1D random walk)

$$\langle x(t)\rangle = 0 \qquad\qquad \langle \Delta x^2(t)\rangle = t \tag{2.11}$$

Therefore each value of $x(t) \sim \mathcal{N}(0, \sqrt{t})$. This means the probability density of the Wiener process is *non-stationary*.

Each solution to the Langevin equation is termed a *realization* and each one is inde-

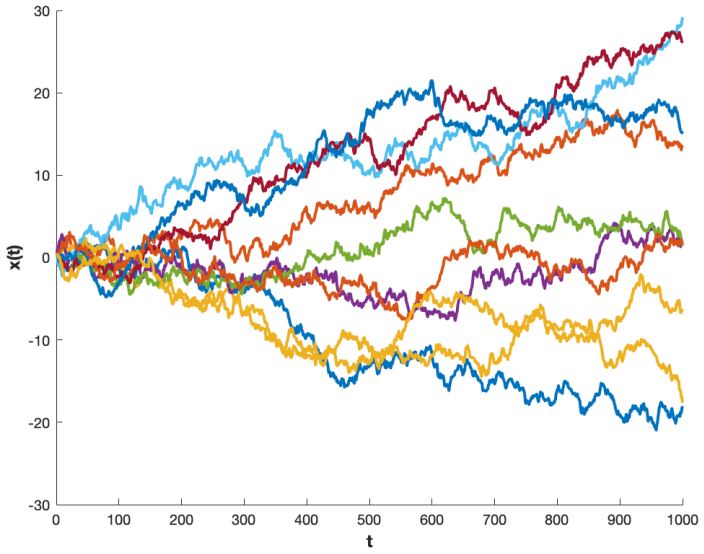

Figure 2.1: Ten independent realizations of the Wiener process, Eqn (2.8). Each increment is from a Gaussian distribution with zero mean and unity variance, $\eta \sim \mathcal{N}(0,1)$. The initial condition is not $x(0) = 0$ but is itself a random number from the same Gaussian distribution.

pendent. Figure 2.1 shows ten realizations of the Wiener process. For completeness, it will be mentioned that the Wiener process is also the description of a free Brownian particle (this was its original derivation).

Ornstein-Uhlenbeck Process

The Langevin equation for the Ornstein-Uhlenbeck process is of the form

$$\dot{x}(t) = -\gamma x(t) + \sigma\eta(t) \tag{2.12}$$

where the drift coefficient is $a(x,t) = -\gamma x(t)$ and the diffusion coefficient is $b(x,t) = \sigma$. The mean and variance can be analytically calculated

$$\langle x(t)\rangle = x_0 e^{-\gamma t} \qquad\qquad \langle \Delta x^2(t)\rangle = \frac{\sigma}{\gamma}(1 - e^{-2\gamma t}) \tag{2.13}$$

The relevance of the OU process as regards neuronal dynamics is it describes *correlated noise* (synonymously called coloured noise). Mathematically, it is equivalent to low-pass filtered white noise. Since synaptic connections are not instantaneous this equation describes the stochastic component of the input current to real neurons.

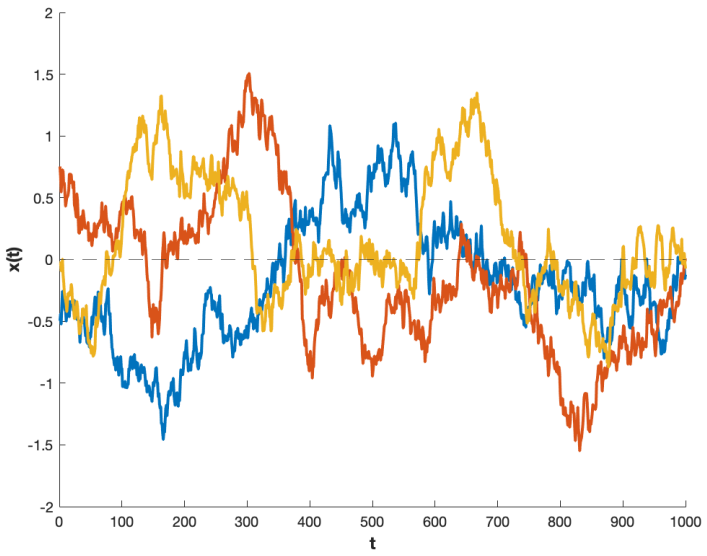

Figure 2.2: Three independent realizations of the Ornstein-Uhlenbeck process, Eqn (2.12). Each increment is from a Gaussian distribution with zero mean and unity variance, $\eta \sim \mathcal{N}(0,1)$. The initial condition is not $x(0) = 0$ but is itself a random number drawn from the same Gaussian distribution.

2.1.3 Fokker-Planck Equation

The FPE describes the time evolution of a continuous *probability density of a stochastic variable*. With the inclusion of synaptic noise the membrane potential $V(t)$ is a stochastic function and $P(V(t), t) \equiv P(V, t)$ is the corresponding density. The most general form of the FPE is given by

$$\partial_t P(V,t) = -\partial_V [a(V,t)P(V,t)] + \frac{1}{2}\partial_V^2 [b(V,t)P(V,t)] \tag{2.14}$$

The first term on the RHS is a *deterministic component* and the second term is a *stochastic component*. For a neuronal population voltage is directly related to input current in that the deterministic term corresponds to mean input current I_0 and the stochastic term to input current noise $\sigma^2\eta$.

For the case of an arbitrary non-zero drift coefficient $a(x,t) = F(V)$ and a vanishing diffusion coefficient $b(x,t) = 0$ the FPE reduces to the *Liouville equation*.

$$\partial_t P(V,t) = \partial_V [F(V)P(V,t)] \tag{2.15}$$

For the case of a vanishing drift coefficient $a(x,t) = 0$ and a non-zero constant diffusion coefficient $b(x,t) = \sigma^2$ the FPE reduces to the standard *diffusion equation*

$$\partial_V P(V,t) = \frac{\sigma^2}{2}\partial_V^2 P(V,t) \tag{2.16}$$

where $D = \sigma/2$. Therefore the full FPE equation is a linear superposition of the Liouville equation and diffusion equation.

2.2 Synaptic Bombardment

Each cortical neuron has approximately 10^4 synaptic connections that release neurotransmitters and create tiny current pulses in a neural 'neighbour'. The random arrival of these *post-synaptic current pulses (PSCPs)* causes the membrane potential in each constituent neuron to *fluctuate asynchronously* and adds a *stochastic noise* component to the input.

Synapses come in two types: *excitatory* or *inhibitory*. A rudimentary description is a single neuron receives synaptic input through the dendrite and passes on synaptic output via the axon. According to *Dale's law* a neuron is classified as being either excitatory or inhibitory depending on its synaptic *output*.

2.2.1 Background Fluctuations

Each synapse has an associated weight or connection strength J. For excitatory synapses $J > 0$ and for inhibitory synapses $J < 0$, by convention. Here consider all synaptic strengths to be equivalent, particularly between inhibitory and excitatory PSCPs, so $|J_E| = |J_I| = \pm J$.

If a neuron is receiving PSCPs from an excitatory population at rate $\nu_E(t)$ and an inhibitory population at rate $\nu_I(t)$, the total input current to the post-synaptic neuron is

$$I(t) = I_0 + \nu_E(t) + \nu_I(t) \tag{2.17a}$$

$$= I_0 + J\sum_i^{N_E} f(t - t_E^i) - J\sum_j^{N_I} f(t - t_I^j) \tag{2.17b}$$

The first sum is over all excitatory spikes K_E and the second sum is over all inhibitory spikes K_I. The spike train is expressed here a general form of *synaptic response function* $f(t-t_{E,I}^{i,j})$, which will be an exponentially decaying PSCP. Taking the expectation value yields

$$\langle I(t)\rangle = I_0 + J\int_{-\infty}^{\infty} dt'\ f(t-t')[\nu_E(t') - \nu_I(t')] \tag{2.18}$$

Note that the integral is a convolution between the two population firing rates and the synaptic response function.

The FPE for this system of two coupled excitatory and inhibitory populations can be expressed in terms of a continuity equation

$$\partial_t P(V,t) = -\partial_V \psi \tag{2.19}$$

with the probability flux given by

$$\psi = P(V,t)\{F(V) + J[\nu_E - \nu_I]\} - \partial_V P(V,t) J^2[\nu_E + \nu_I] \tag{2.20}$$

Explicitly the FPE is given by

$$\partial_t P(V,t) = -\partial_V\{P(V,t)[F(V) + J[\nu_E - \nu_I]] - \partial_V P(V,t) J^2[\nu_E + \nu_I]\} \tag{2.21}$$

In this form it becomes clear that the first term on the RHS is related to mean input through $J[\nu_E - \nu_I]$ and the second term is related to input variance through $J^2[\nu_E + \nu_I]$.

2.2.2 Diffusion Approximation

The main source which keeps a population in a non-arbitrary *asynchronous* state is background noise. This noise has the effect of leading to diffusion-type dynamics for the population density. That is because synaptic bombardment is a random process which follows Poisson statistics, but for large number of spikes (exact as $lim\ n \to \infty$) they can be approximated to by a Gaussian distribution. This allows a stochastic trajectory to be modelled as a diffusive process with fluctuations.

For a large number of random synaptic inputs with small amplitude PSCPs compared with the firing threshold, the total input current can be approximated as a mean input

current component plus a random Gaussian fluctuation component.

$$I(t) = I_0 + \sigma\eta(t) \qquad\qquad \eta(t) \sim \mathcal{N}(0,1) \tag{2.22}$$

Here I_0 is mean input current, σ is the magnitude of random fluctuations, and $\eta(t)$ is a Gaussian distributed random variable. Characterization of the current only requires the mean $\langle I(t)\rangle$ and the covariance $\langle \delta I(t)\delta I(t')\rangle$ where $\delta I(t) = I(t) - \langle I(t)\rangle$.

$$\langle \delta I^2(t)\rangle = J^2 \int_\infty^\infty dt' \int_\infty^\infty dt''\ f(t-t')f(t-t'')[\nu_E(t') - \nu_I(t')] \tag{2.23}$$

2.2.3 Gaussian White Noise

$\eta(t)$ is termed a *general stochastic process.* If synaptic transmission is taken to be instantaneous then the signal generated by PSCPs will be delta functions and their random arrival at the post-synaptic neuron described by *Poisson statistics.* Importantly, using the diffusion approximation one can describe the fluctuations caused by instantaneous PSCPs using a normalized Gaussian distribution with zero mean and $\sigma^2 t$ variance.

Mathematically, Gaussian white noise is the derivative of the Wiener process

$$\eta(t) = \frac{dW(t)}{dt} \tag{2.24}$$

Any variable which depends on $\eta(t)$ is *Markovian* if and only if $\eta(t)$ is Gaussian distributed. The mean and covariance are respectively given by

$$\langle \eta(t)\rangle = \left\langle \frac{dW(t)}{dt} \right\rangle = 0 \tag{2.25a}$$

$$\langle \eta(t)\eta(t')\rangle = \left\langle \frac{dW(t)}{dt}\frac{dW(t')}{dt'} \right\rangle = \sigma^2\delta(t-t') \tag{2.25b}$$

For $t \neq t'$, $\langle \eta(t)\eta(t')\rangle = 0$ and each $\eta(t)$ is *independently and identically distributed (i.i.d.).* However for $t = t'$, $\langle \eta^2(t)\rangle \to \infty$. Figure 2.3 displays three realizations of Gaussian white noise.

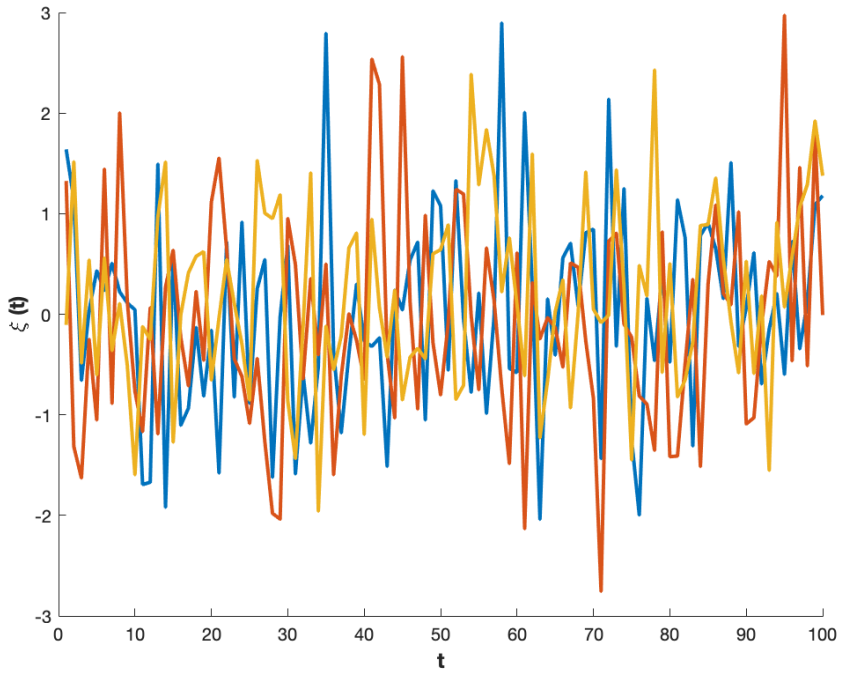

Figure 2.3: Three independent realizations of Gaussian white noise. $\xi(t)$ on the y-axis is equivalent to $\eta(t)$ as used in these notes. Technically these are just a series of points, but are shown here connected with lines for clarity and to highlight that this stochastic function is not strictly differentiable.

2.2.4 Coloured Noise

Physically synaptic signalling is not instantaneous because the release/binding of neurotransmitters from/to the pre-/post-synaptic neuron are biochemical processes. Therefore to remain a valid approximation, treating a PSCP as a step function with exponential decay requires an associated non-zero time constant τ_c. The subscript is explained by the preferred terminology of *correlation time* for the effective timescale.

This type of input fluctuations is termed *coloured noise*, in contrast to white noise, because it has an attenuated power spectral density. It is also simply called *correlated noise* and the time constant denoted τ_c instead. The Langevin equation which describes coloured noise is that of the Ornstein-Uhlenbeck process Eqn (2.12), but usually expressed in slightly different form for the current

$$\tau_c dI(t) = [I_0 - I(t)]dt + \sqrt{t}\sigma dW(t) \tag{2.26}$$

The OU process is mean-reverting; the larger the deviation from the mean I_0 the larger $[I_0 - I(t)]$. This is why in Fig 2.2 the realizations diffuse move symmetrically about the zero mean.

The expressions for mean and covariance of the OU process variable, in this case input current, can be analytically calculated

$$\langle I(t) \rangle = 0 \tag{2.27a}$$

$$\langle I(t) I(t') \rangle = \frac{\sigma^2}{2} e^{-|t-t'|/\tau_c} \tag{2.27b}$$

Since covariance only depends on the *difference* in times $(t - t')$ a stationary solution for probability density of the OU process exists.

N.B. Technically Gaussian white noise is *delta-function correlated*. This detail is usually ignored and white noise is referred to as *uncorrelated* to directly contrast with coloured noise which is *correlated* in the general sense. The white noise case is always recovered from the coloured noise case when correlation time goes to zero, $lim\ \tau_c \to 0$. Comparing Eqns (2.25b) & (2.27b) should help clarify the distinction.

2.2.5 Encoding Channels

The *mean channel* $\langle I \rangle$ is a measure of excitatory/inhibitory balance and the *variance channel* is a measure of overall activity.

$$\langle I \rangle \sim (\nu_E - \nu_I) \qquad \textbf{mean-channel} \tag{2.28a}$$

$$\langle \delta I^2 \rangle \sim (\nu_E + \nu_I) \qquad \textbf{variance-channel} \tag{2.28b}$$

A neuron can be driven either by positive or negative differences in the relative ν_E/ν_I firing rates. (To be clear, here $\delta I^2 = \sigma^2$, but is used for consistency with later sections.) Consider a change in firing rates of magnitude A.

In the mean-channel encoding scheme the increased firing-rate of excitatory neurons, $+A$, and the decreased activity of inhibitory neurons, $-A$, results in $\Delta I \neq 0$ and

$\Delta\delta I^2 = 0$.

$$I \to (\nu_E + A) - (\nu_I - A) \qquad \Delta I = 2A \tag{2.29a}$$
$$\delta I^2 \to (\nu_E + A) + (\nu_I - A) \qquad \Delta\delta I^2 = 0 \tag{2.29b}$$

In the variance-channel encoding scheme an increased firing rate of both excitatory and inhibitory neurons, $+A$, results in $\Delta I = 0$ and $\Delta\delta I^2 \neq 0$.

$$I \to (\nu_E + A) - (\nu_I + A) \qquad \Delta I = 0 \tag{2.30a}$$
$$\delta I^2 \to (\nu_E + A) + (\nu_I + A) \qquad \Delta\delta I^2 = 2A \tag{2.30b}$$

Asymmetric changes in the ν_E/ν_I firing rates are only tracked in the mean-channel. *Symmetric* changes to ν_E/ν_I are tracked only via the variance-channel.

The input current can be written as a deterministic constant component, given by the mean, and a stochastically varying component, given by the variance.

$$I(t) = I_0 + \delta I(t) \tag{2.31}$$

$\delta I(t)$ is referred to as synaptic *noise*. The generalized IF model equation of motion can be expressed as

$$\dot{V}(t) = F(V(t)) + I(t) \tag{2.32a}$$
$$= F(V(t)) + J[\nu_E - \nu_I] + J^2[\nu_E + \nu_I]\eta(t) \tag{2.32b}$$
$$= F(V(t)) + I_0 + \delta I(t) \tag{2.32c}$$

where the relation between excitatory/inhibitory firing rates and mean input $I_0 = J(\nu_E - \nu_I)$ and input variance $\delta I(t) = J^2(\nu_E + \nu_I)$ has been used.

2.3 Stochastic Firing Rates

If neuronal populations are a 'computational unit' then how quickly they can change from one state to another determines the speed of computation. Decomposition of the input current into a mean component, which can be time-dependent, and a noise component, which are fluctuations about that mean, is the fundamental paradigm needed

to describe population dynamics in real neurons. By setting $\delta I(t) = \sigma\eta(t)$ this type of input

$$I(t) = I_0(t) + \sigma\eta(t) \qquad \eta(t) \sim \mathcal{N}(0,1) \qquad (2.22\ ^*)$$

is referred to as *noisy input* regardless if the mean is zero or non-zero. The $I_0(t)$ term is a *deterministic* contribution and the $\sigma\eta(t)$ term is a *stochastic* contribution where σ is a measure of fluctuation amplitude and $\eta(t)$ is Gaussian white noise.

2.3.1 Realization-Density Equivalence

The dynamics of a *single* neuron are described by SDEs and the dynamics of a population of neurons are described by the FPE. For a single neuron with noisy input *membrane potential* follows

$$dV = [F(V) + I_0]dt + \sigma dW \qquad (2.33)$$

where the dt term is the *deterministic component* and dW is the *stochastic component*; specifically the Wiener increment. Because of the random nature of the Wiener process each solution is different and referred to as a *realization*.

For a neuronal population with noisy input *probability density* evolves according to

$$\partial_t P(V,t) = -\partial_V \left\{ [F(V) + I_0]P(V,t) - \frac{\sigma^2}{2}\partial_V P(V,t) \right\} \qquad (2.34)$$

where the first-order partial derivative term is the *deterministic drift component* and the second-order partial derivative term is the *stochastic diffusion component*.

Advection Equation

As an example, consider the case when $F(V) = c$ where c is some voltage-independent constant. From the single neuron perspective membrane potential follows

$$V(t) = [c + I_0]t + \sigma W(t) \qquad (2.35)$$

where $W(t)$ is the Wiener process. This is obtained by integrating Eqn (2.33) and using the initial condition $V(0) = 0$. To further simplify c can be absorbed into the value of I_0.

From the neuronal population perspective density follows Eqn (2.34), but the first term vanishes since $\partial_V(c + I_0) = 0$ leaving

$$\partial_t P(V,t) = -\frac{\sigma^2}{2}\partial_V^2 P(V,t) \tag{2.36}$$

which is the standard *diffusion equation* with $D = \sigma^2/2$. The solution is a normalized Gaussian with initial condition

$$P(V,t) = \frac{1}{\sqrt{2\pi\sigma^2}}\exp\left(\frac{-V^2}{2\sigma^2 t}\right) \qquad P(V,0) = \delta(V) \tag{2.37}$$

Conditional Probability

Question: The FPE can be derived from the SDE so an ensemble of realizations allows for a calculation of the density. If the number of neurons in the ensemble $\longrightarrow \infty$ this becomes exact. However, knowing the full density solution to the FPE can individual realizations be obtained?

A conditional probability describes the density at the point (V,t) given that earlier the system was at point (V_0,t_0) and is denoted $P(V,t|V_0,t_0)$. For the above example of the diffusion equation Eqn (2.37) the conditional probability and initial condition are

$$P(V,t|V_0,t_0) = \frac{1}{\sqrt{2\pi\sigma^2}}\exp\left(\frac{-(V-V_0)^2}{2\sigma^2(t-t_0)}\right) \qquad P(V,t_0|V_0,t_0) = \delta(V-V_0) \tag{2.38}$$

Take the path of a single neuron realization and discretize it into n steps such that the overall process goes from $(V_0,t_0) \longrightarrow (V_n,t_n)$ moving through the subsequent set of points $\{V_0,t_0;V_1,t_1;\ldots;V_{n-1},t_{n-1};V_n,t_n\}$. A *realization is now described by the path of conditional density* through these same points

$$P(V_1,t_1|V_0,t_0) \longrightarrow P(V_2,t_2|V_1,t_1) \longrightarrow \cdots\cdots \longrightarrow P(V_n,t_n|V_{n-1},t_{n-1}) \tag{2.39}$$

That is, to obtain a realization from conditional density one must choose random numbers from the Gaussian distribution describing the diffusion.

2.3.2 Integrate-and-Fire Models

The generalized linear *integrate-and-fire (IF)* model has the equation of motion

$$\dot{V(t)} = F(V(t)) + I_{ext}(t) \tag{2.40}$$

There are three standard forms of IF models with different voltage dependence

$$F(V(t)) = \begin{cases} V(t) & \text{LIF} \\ V^2(t) & \text{QIF} \\ \sim e^{V(t)} & \text{EIF} \end{cases} \tag{2.41}$$

These are respectively called the *leaky, quadratic,* and *exponential* IF models. They constitute a class of neuron models (IF) separate from the conductance-based models (CBM) of the Hodgkin-Huxley and Morris-Leccar variety.

In § 2.3.3 the LIF is introduced and numerically simulated; its dynamics are representatively shown in Fig 2.5. The QIF model was briefly discussed with reference to derivation of the *normal form* or phase representation in § 1.3.1. The specifics of the EIF model are omitted here, but it is often considered the most robust in terms of reproducing spike initiation dynamics.

HOMEWORK PROBLEM: Does the EIF model have $\nu_{EIF} \propto \ln^{-1}(I_{ext})$ or $\nu_{EIF} \propto I_{ext}^{-1/2}$? HINT: The EIF model describes a system undergoing a SNIC bifurcation at the onset of firing; the exact equation of motion is not needed.

Phase Representation

A 1D *phase representation* constitutes the state of the neuron by an angle ϕ. Changes to the membrane potential are realized as movement on a circle with some arbitrary angle being defined as rest ($\phi = 0$) and another as defining a spiking event ($\phi = 2\pi$). Note the periodic reset $\phi(0) = \phi(2\pi)$. (Another convention is to use $\pm\pi$ as the two values.) Explicitly

$$\dot{\phi}(t) = \omega_0 + G(I_{ext}(t)) \tag{2.42}$$

where ω_0 is a constant and $G(I_{ext}(t))$ is some function of the driving current.

In a 1D system there is always a valid transformation to a circular coordinate system. Consider the mapping from voltage V to the new state variable ϕ of the form $\phi = h(V)$. Then

$$\begin{aligned}
\dot{\phi} &= h'(V)\dot{V} && \text{(2.43a)}\\
&= h'(V)[F(V) + I_{ext}(t)] && \text{(2.43b)}\\
&= h'(V)F(V) + h'(V)I_{ext}(t) && \text{(2.43c)}\\
&\equiv \omega_0 + G(I_{ext}(t)) && \text{(2.43d)}
\end{aligned}$$

where the definition is valid because $h'(V)$ is some unspecified function.

For stationary input $G(I_{ext}(t)) = 0$ and $\dot{\theta} = \omega_0$. The FPE becomes

$$\partial_t P(\phi, t) = -\omega \partial_\theta P(\theta, t) \tag{2.44}$$

The firing rate is proportional to the probability density at (an arbitrarily defined) spiking angle ϕ_S.

$$\nu(t) = \omega_0 P(\phi_S, t) \tag{2.45}$$

A more detailed discussion of IF models is an entire subject in itself, but one facet that is crucial to modeling spiking is a *hard threshold* and *reset condition*. It allows $\nu(t)$ to equal the probability flux through an absorbing boundary.

Question: Can a non-uniform population firing rate (refer to Fig 2.4(left)) occur if the identical constituent neurons get stationary input or does this indicate that the input is varying?

Mathematically, $P(\phi_S, t)$ is arbitrary and can simply be given any shape which results in a congruent firing rate pattern. Said differently, if a single neuron is being driven over the periodic interval $[0, 2\pi]$ and the point at which spiking occurs ϕ_S can be chosen, it can be done so in such a way that any overall firing pattern results; illustrated in Fig 2.4(right). *Note that this is not what happens in the brain.* In real populations the neurons receive sparse asynchronous inputs which makes them fire stochastically.

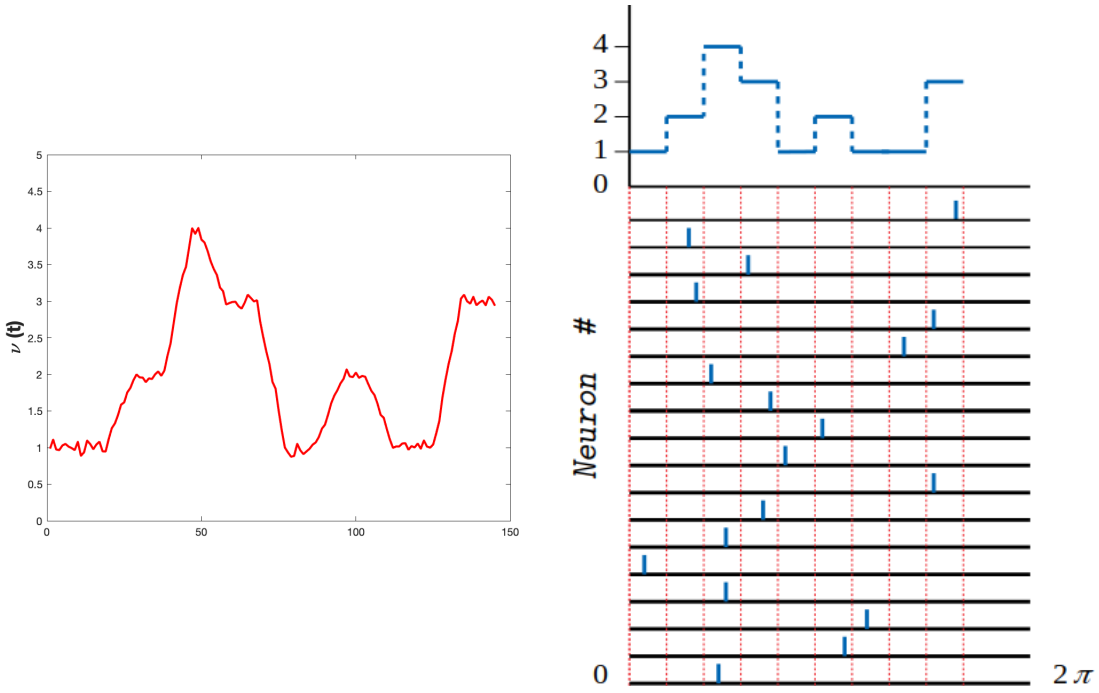

Figure 2.4: (left) Hypothetical population firing rate with a trivial timescale. **(right)** Each neuron - black line - fires one spike over the period 0 to 2π. These spikes are then added together to get a total firing rate. The stepped blue trace can be thought of as an arbitrarily chosen $P(\theta_S, t)$ which would give rise to the $\nu(t)$ line shown in red. The discrete binning is for illustrative purposes.

2.3.3 Threshold and Reset

The IF equations of motion, Eqns (2.40) & (2.41), are insufficient to describe spiking activity. They must be supplemented with an *absorbing boundary* at threshold V_T and a reset to rest V_R immediately after the spike. (For simplicity, the rest potential and reset potential are taken to be equal.) Conceptually, whenever the membrane potential reaches threshold a 'spike' occurs and it is instantly reset to a hyper-polarized value. Denoting the time a spike occurs as t^f

$$V(t^f) \equiv V_T \qquad \textbf{hard threshold} \tag{2.46a}$$

$$V(t^f + \varepsilon) \equiv V_R \qquad \textbf{reset condition} \tag{2.46b}$$

A numerical simulation for one realization of the LIF model using a threshold and reset condition is shown in Fig 2.5. The equation of motion for the membrane potential is $\dot{V}(t) = -V(t) + I(t)$ where the input current is described by the OU process of Eqn (2.26).

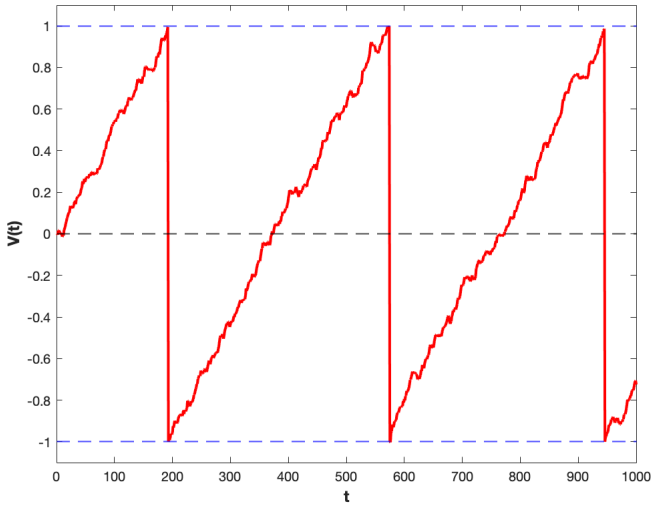

Figure 2.5: A numerical example of the leaky integrate and fire model with threshold $V_T = 1$ and reset $V_R = -1$. The input current is described by the Ornstein-Uhlenbeck equation, Eqn (2.26) with $I_0 = 0.005, \sigma = 0.5, \tau_c = 0.5, \tau_m = 1$ in arbitrary units. The initial condition $V(0) = 0$ was chosen for clarity. The voltage increases deterministically with stochastic fluctuations (noise) until reaching threshold when a 'spike' is registered and the potential is reset.

2.3.4 Detailed Balance

Question: For the case of Gaussian white noise do the density dynamics $P(V,t)$ for the state variable $V(t)$ describe a population of spiking neurons? Asked differently, can a stochastic system exhibit detailed balance?

A stationary density $P(V,t) \to P_0(V)$ satisfies the condition

$$\partial_t P(V,t) = \partial_t P_0(V) = 0 \tag{2.47}$$

The FPE for this system is

$$\partial_t P(V,t) = -\partial_V \left\{ [F(V) + I_0]P(V,t) - \frac{\sigma^2}{2}\partial_V P(V,t) \right\} \tag{2.48}$$

where the probability flux is explicitly

$$\psi(V,t) = [F(V) + I_0]P(V,t) - \frac{\sigma^2}{2}\partial_V P(V,t) \tag{2.49}$$

There are two ways stationarity, Eqn (2.47), can be satisfied. Either the probability flux, as given by Eqn (2.49), is zero such that the drift term cancels with the diffusion term

$$\psi(V,t) = 0 \tag{2.50a}$$

$$[F(V) + I_0]P(V,t) = \frac{\sigma^2}{2}\partial_V P(V,t) \tag{2.50b}$$

or the probability flux is constant ($= c$) in voltage such that the partial derivative with respect to V is zero.

$$\psi(V,t) \longrightarrow \psi(t) \qquad \partial_V \psi(V,t) = \partial_V \psi(t) = 0 \qquad \therefore \;\; \psi(t) = c \tag{2.51}$$

The first scenario, Eqn (2.50), corresponds to the system being in detailed balance; the total flux in the $\pm$ directions are equal in magnitude. A spiking neuron model can only hold this equality for *reflecting boundaries* at threshold and reset, which is physically invalid.

The second scenario, Eqn (2.51), describes a non-zero probability flux for a population that *can* spike. This is attained if the boundary at V_T is an *absorbing boundary*. The effect of an absorbing boundary is to remove neurons that have spiked from the population thereby lowering the density. To maintain a constant probability flux there must be an influx at V_R, termed *reinjection*.

If absorption at V_T equals reinjection at V_R this implies periodic boundary conditions since the density is conserved; becoming exact in $lim\ V_T \to \infty$ and $lim\ V_R \to -\infty$.

$$\partial_t P(V,t)\Big|_{V_T} = \partial_t P(V,t)\Big|_{V_R} \tag{2.52}$$

2.4 Fluctuation-Driven Regime

Neuronal populations jointly engaged in a single, but dynamic, task have different inputs arriving at this 'processing unit' and must quickly change their collective state to relay information. This input/output paradigm is studied in the *fluctuation-driven regime* where neurons are bombarded with uncorrelated synaptic inputs that induce firing (by noise).

Because the probability density describes a high-dimensional system, it is a continuous function of time and as a field theory has infinitely many degrees of freedom. Therefore a complete description of the dynamic response requires *mean field theory*. The standard method of analysis uses *linear response theory* with perturbations to the FPE. The result is a complete first-order description of population response, with which the conditions that make this response (ultra)fast can be investigated.

2.4.1 Frequency Response

To directly examine the effects of changes to mean- and variance-input current consider the linear expansions

$$I(t) = I_0 + \delta I(t) \qquad \delta I(t) \ll I_0 \tag{2.53a}$$

$$\sigma^2(t) = \sigma_0^2 + \delta\sigma^2(t) \qquad \delta\sigma^2(t) \ll \sigma_0^2 \tag{2.53b}$$

The subscript 0 denotes *stationary* terms and the δ term is small changes in time. Note that $\delta\sigma^2$ is not a variance in itself therefore it can be positive or negative.

Using these new representations, the population firing rate $\nu(I, \sigma^2, t)$ might be assumed to follow

$$\nu(t) = \nu_0 + \frac{\partial \nu}{\partial I}\delta I(t) + \frac{\partial \nu}{\partial \sigma^2}\delta\sigma^2(t) + \mathcal{O}(\cdots)$$

but due to the non-linear dynamics of the population firing rate, **this is incorrect**.

Instead, the first-order corrections to the population firing rate require convolutions with Green's functions

$$\nu(t) = \nu_0 + \int_{-\infty}^{\infty} d\tau\ G_I(t-\tau)\delta I(t) + \int_{-\infty}^{\infty} d\tau\ G_{\sigma^2}(t-\tau)\delta\sigma^2(t) \tag{2.54}$$

These Green's functions are non-trivial to calculate, but what is important is their general form. The first integral should be interpreted as a change to mean input $\delta I(t)$ will cause a change to the firing rate $\nu(t)$ by an amount proportional to G_I. Likewise, the second term means a change to input variance $\delta\sigma^2(t)$ will change the firing rate $\nu(t)$ by an amount proportional to G_{σ^2}.

This first-order approximation is valid as long as the integral terms are of the same order of magnitude as the stationary firing rate ν_0. Using terminology from *linear response theory* these Green's functions are referred to as *impulse response functions*.

Writing the population firing rate as $\nu(t) = \nu_0 + \delta\nu(t)$ where $\delta\nu(t)$ is the two integral terms in Eqn (2.54) and taking the Fourier transform

$$\tilde{\delta\nu} = \tilde{G}_I(\omega)\tilde{\delta I}(\omega) + \tilde{G}_{\sigma^2}(\omega)\tilde{\delta\sigma^2}(\omega) \tag{2.55}$$

In the Fourier domain the terms $\tilde{G}(\omega)$ are called *frequency response functions*. In particular $|\tilde{G}(\omega)|$ is referred to as *dynamic gain*.

One special case is that of *perfect fidelity* when $\tilde{G}_I = \tilde{G}_{\sigma^2} = c$ where c is some constant; the dynamic gain is now frequency-independent. Physically this cannot be true - it would represent superconducting neurons capable of tracking inputs at arbitrarily high frequencies.

Another special case is that of a *generator potential* with

$$\tilde{G}_I \propto \frac{1}{1 + i\omega\tau_m} \qquad\qquad f_{cutoff} = \frac{1}{2\pi\tau_m} \tag{2.56}$$

where τ_m is the characteristic time constant of the cell membrane. This form of frequency response is frequency-dependent and for $2\pi\omega > f_{cutoff}$ the response is heavily attenuated (*i.e.* low-pass filtered). Passive properties of the cell membrane determine what frequencies are affected.

2.4.2 Linear Perturbation Theory

Using standard perturbation theory perform a power-series expansion of the probability density with a small deviation characterized by $\varepsilon \ll 1$

$$P_\varepsilon(V,t) = P_0(V) + \varepsilon P_1(V,t) + \varepsilon^2 P_2(V,t) + \mathcal{O}(\cdots) \tag{2.57}$$

where $P_0(V)$ is the *stationary density*. This is exact in the *lim* $\varepsilon \to 0$.

Mean Perturbation

First consider a small perturbation to the mean input current

$$I(t) = I_0 + \varepsilon\delta I(t) \tag{2.58a}$$
$$\sigma^2(t) = \sigma_0^2 \tag{2.58b}$$

(A perturbation to the noise $\varepsilon\delta\sigma^2(t) \neq 0$ will be considered subsequently.) Using this expression for $P_\varepsilon(V,t)$ in the FPE, Eqn (2.48), gives for the LHS

$$\partial_t P_\varepsilon(V,t) = \varepsilon\partial_t P_1(V,t) + \varepsilon^2\partial_t P_2(V,t) + \mathcal{O}(\cdots) \tag{2.59}$$

and for the RHS

$$\begin{aligned} -\partial_V\{&[F(V) + I_0 + \varepsilon\delta I(t)][P_0(V) + \varepsilon P_1(V,t) + \varepsilon^2 P_2(V,t) + \mathcal{O}(\cdots)] \\ &- \frac{\sigma_0^2}{2}\partial_V[P_0(V) + \varepsilon P_1(V,t) + \varepsilon^2 P_2(V,t) + \mathcal{O}(\cdots)]\} \end{aligned} \tag{2.60}$$

The first-order correction $P_1(V,t)$ is obtained by setting linear terms in ε from Eqn (2.59) equal to linear terms in ε from Eqn (2.60).

$$\partial_t P_1(V,t) = -\partial_V\left\{[F(V) + I_0]P_1(V,t) - \frac{\sigma_0^2}{2}\partial_V P_1(V,t)\right\} + \delta I(t)\partial_V P_0(t) \tag{2.61}$$

Note that this is of the same form as the unperturbed FPE with addition of a $\delta I(t)\partial_V P_0(t)$ term; which can be considered a 'driving' term. If $\delta I(t) = 0$ this is a transport equation for the probability flux and the integral of $P_1(V,t)$ is a constant of motion. However, if $\delta I(t) \neq 0$ then $P_1(V,t)$ is not a probability in the strict sense that it can be either $\pm$.

The population firing rate *equals the probability flux at the absorbing boundary.* Expressed as a first-order correction to the stationary rate

$$\nu(t) = \nu_0 + \varepsilon\nu_1(t) \tag{2.62}$$

An absorbing boundary at threshold V_T requires $P(V_T,t) = 0$, since it is a smooth function. The first-order correction is

$$\nu_1(t) = [F(V) + I_0]P_1(V_T,t) - \frac{\sigma_0^2}{2}\partial_V P_1(V_T,t) + \delta I(t)P_0(V_T) \tag{2.63}$$

where density is evaluated at the absorbing boundary. Since $P_0(V_T) = P_1(V_T, t) = 0$ the first and third term vanish, leaving

$$\nu_1(t) = -\frac{\sigma_0^2}{2}\partial_V P_1(V_T, t) \tag{2.64}$$

The correction to the firing rate is proportional to the slope of $P_1(V_T, t)$ and is *independent* of $\delta I(t)$. Therefore changes to mean input current only affect the stationary firing rate ν_0.

Variance Perturbation

Instead consider a small perturbation to the input current variance

$$I(t) = I_0 \tag{2.65a}$$
$$\sigma^2(t) = \sigma_0^2 + \varepsilon\delta\sigma^2(t) \tag{2.65b}$$

The LHS of the FPE using $P_\varepsilon(V, t)$ remains the same as above

$$\partial_t P_\varepsilon(V, t) = \varepsilon\partial_t P_1(V, t) + \varepsilon^2\partial_t P_2(V, t) + \mathcal{O}(\cdots) \tag{2.59*}$$

with the RHS now given by

$$\begin{aligned} -\partial_V\{&[F(V) + I_0][P_0(V) + \varepsilon P_1(V, t) + \varepsilon^2 P_2(V, t) + \mathcal{O}(\cdots)] \\ &- \frac{\sigma_0^2 + \varepsilon\delta\sigma^2(t)}{2}\partial_V[P_0(V) + \varepsilon P_1(V, t) + \varepsilon^2 P_2(V, t) + \mathcal{O}(\cdots)]\} \end{aligned} \tag{2.66}$$

Again calculating the equation for $P_1(V, t)$ by equating linear terms of ε in Eqns (2.59) & (2.66) yields an expression for the first-order density correction

$$\partial_t P_1(V, t) = -\partial_V\left\{[F(V) + I_0]P_1(V, t) - \frac{\sigma_0^2}{2}\partial_V P_1(V, t) - \frac{\delta\sigma^2(t)}{2}\partial_V P_0(V)\right\} \tag{2.67}$$

The first-order correction to population firing rate is still the flux into the absorbing boundary

$$\nu_1(t) = [F(V) + I_0]P_1(V_T, t) - \frac{\sigma_0^2}{2}\partial_V P_1(V_T, t) - \frac{\delta\sigma^2(t)}{2}\partial_V P_0(V_T) \tag{2.68a}$$

$$= -\frac{\sigma_0^2}{2}\partial_V P_1(V_T, t) - \frac{\delta\sigma^2(t)}{2}\partial_V P_0(V_T) \tag{2.68b}$$

where the first term again vanishes because $P_1(V_T, t) = 0$. The remaining $\partial_V P_1$ is a deterministic term, but the $\partial_V P_0$ term is an instantaneous response term. This is because $\partial_V P_0 \sim \nu_0$ so the last term is $\sim \delta\sigma^2(t)\nu_0$. Therefore changes of variance will be instantly recorded as changes in firing rate. As presented, the *variance-channel is instantaneous*; it can track changes to the input statistics up to arbitrarily high frequencies.

Fick's law states that probability flux will be proportional to the diffusion coefficient times divergence of the density (where noise plays the role of the diffusion term).

$$\psi \propto \sigma^2 \partial_V P(V, t) \tag{2.69}$$

Comment on Linear Response Functions

A change to mean input, $\delta I(t)$, or to input variance, $\delta\sigma^2(t)$, alters firing rate $\nu(t)$ as given by Eqn (2.54), which was

$$\nu(t) = \nu_0 + \int_{-\infty}^{\infty} d\tau\ G_I(t-\tau)\delta I(t) + \int_{-\infty}^{\infty} d\tau\ G_{\sigma^2}(t-\tau)\delta\sigma^2(t) \tag{2.54*}$$

The terms $G_I(t)$ and $G_{\sigma^2}(t)$ are *Green's functions*, but in this context are referred to as linear response functions. Using linear perturbation theory, *general* expressions were given for first-order mean-channel and variance-channel perturbations. A direct calculation requires knowledge of $P_0(V_T)$ and $P_1(V_T, t)$.

However, these terms are highly intractable and calculating a closed form expression is not possible under most circumstances. Omitting the details, methods for measuring impulse response functions are based on different outputs from three types of input:

i) delta impulse, $I(t) = \delta(t) \longrightarrow G(t)$
ii) sinusoidal input, $I(t) = \sin(\omega t) \longrightarrow \tilde{G}(\omega) \xrightarrow{\mathcal{F}^{-1}} G(t)$
iii) step current, $I(t) = \theta(t) \longrightarrow G'(t) \xrightarrow{\partial_t} G(t)$

Often the more useful expression for linear response functions is in the frequency domain, $\tilde{G}(\omega)$. In this form spectral density can be analyzed since at frequencies below the cutoff, input/output fidelity is near unity. For $2\pi\omega_c > f_{cutoff}$ input/output fidelity diminishes. (There are resonant peaks when certain selective frequncy bands are amplified, but this phenomenon will not be further discussed here.) In § 2.5.4 a full derivation of $\tilde{G}(\omega)$ is performed.

The Green's function is *not a property of the neuron.* An example of a biophysical property is ion channel conductivity. Instead, *Green's functions depend on the working point.* For a neural population there are different impulse response functions depending on the working point. Mathematically, first-order perturbation theory is a linearization and it strongly matters *where in state space this linearization is performed.* When input statistics (*e.g.* frequency composition) are changed the impulse response function will be modified.

2.4.3 Correlated Noise Dynamics

Question: For Gaussian white noise there is an instantaneous response in the variance-channel. What happens if the synapses are made more realistic and use correlated (coloured) noise instead? Will either the mean- or variance-channel elicit an instantaneous response?

Two SDEs describe the membrane potential and input current for correlated (coloured) noise, respectively

$$dV = [F(V) + I(t)]dt \tag{2.70a}$$

$$dI = \frac{I_0 - I(t)}{\tau_c}dt + \sigma dW \tag{2.70b}$$

where σ is noise fluctuation amplitude and dW is the Wiener increment as defined in Eqn (2.8). A pre-synaptic spike causes a step-function post-synaptic current pulse that decays with characteristic timescale τ_c such that the PSCP $\sim \theta(t)e^{-t/\tau_c}$.

Probability density is now a function of membrane voltage, input current, and time

$P(V, I, t)$ with corresponding *two-dimensional* FPE

$$\partial_t P(V,I,t) = \\ -\partial_V \left\{[F(V)+I]P(V,I,t)\right\} - \partial_I \left\{ \left[\frac{I_0 - I}{\tau_c}\right] P(V,I,t) - \frac{\sigma^2}{2}\partial_I P(V,I,t) \right\} \tag{2.71}$$

The density must satisfy the boundary conditions

$$\lim_{I\to\pm\infty} P(V,I,t) \longrightarrow 0 \tag{2.72a}$$

$$P(V_T,I,t) \neq 0 \tag{2.72b}$$

At threshold the density no longer needs to go to zero. Now all of the noise is in the current component and the ∂_V term is independent of noise. Therefore $P(V, I, t)$ must be smooth in the $I-$direction, but in the $V-$direction the density can be non-zero arbitrarily close to threshold, with an instantaneous reduction to zero at threshold.

The firing rate is still given by flux perpendicular to the absorbing boundary in the $VI-$plane.

$$\nu(t) = \int_\infty^\infty dI \ [F(V) + I(t)]P(V_T, I, t) \tag{2.73}$$

In the *mean-channel* using linear perturbation theory to write first-order corrections

$$I(t) = I_0 + \varepsilon\delta I(t) + \mathcal{O}(\cdots) \tag{2.74a}$$

$$P(V,I,t) = P_0(V,I) + \varepsilon P_1(V,I,t) + \mathcal{O}(\cdots) \tag{2.74b}$$

yields the first-order correction to firing rate

$$\nu_1(t) = \int_\infty^\infty dI \ \left\{\delta I(t) P_0(V_T, I) + [F(V_T) + I_0]P_1(V_T, I, t)\right\} \tag{2.75}$$

For white noise the first term vanished and changes to mean input current deterministically altered the stationary firing rate. However, in the correlated noise case the $\delta I(t)P_0$ term effects ν_1 and therefore deviations of mean input current have a (weak) instantaneous effect on $\nu(t)$.

With correlated currents, voltage trajectories become smooth functions of time. In the absence of a driving current component there will be many sample paths (*i.e.* neu-

rons) that fluctuate close to threshold without spiking. An infinitesimal input can now instantaneously push them across threshold and generate spikes which are temporally very precise.

N.B. The calculation for a variance-channel perturbation and resulting first-order correction to firing rate for correlated noise *will not be described* in these notes. Analogous to the white noise case, ν_1 will contain a factor $\delta\sigma^2(t)P_0(V, I, t)$ which means the output can instantaneously track changes to the input up to arbitrarily high frequencies.

2.5 Gauss-Rice Theory

The foundation of this model is the probability density *must* be Gaussian distributed (as the name suggests). However, a Gaussian only goes to zero in the infinite limits and the absorbing boundary condition requires $P(V_T, t) = 0$.

Consider a population of neurons subject to asynchronous synaptic bombardment - being in the fluctuation-driven regime. Voltage realizations $V(t)$ are erratic random functions of time, but these trajectories are described by a *Gaussian random function*

$$P(V) \sim \exp\left(-\frac{V_T - V_0}{2\sigma_V^2}\right) \tag{2.76}$$

Said differently, the each of the voltage fluctuations are *i.i.d* Gaussian. This becomes a spiking model by defining a *non-absorbing* boundary condition (*i.e.* no reset condition) and registering positive-slope threshold crossing as 'spikes'. Excursions of voltage above threshold are not treated any differently as they will be small and of short duration (*i.e.* usually the voltage will be below threshold).

Density is now a random functional of a random function, $P[V(t), t]$. Calculation of firing rate requires counting of positive-slope threshold crossings over an ensemble. The number of threshold crossing N of the random function $V(t)$ over an interval T is given

by

$$N = \int_{-T/2}^{T/2} dt\ \delta(V(t) - V_T)|\dot{V}(t)| \tag{2.77a}$$

$$= \sum_{t^f}^{K} \frac{1}{|\dot{V}(V_T)|}|\dot{V}(t)| \tag{2.77b}$$

$$= \sum_{t^f}^{K} 1 \tag{2.77c}$$

$$= \int_{-T/2}^{T/2} dt\ \delta(V(t) - V_T)\ \dot{V}(t)\ \theta(\dot{V}(t)) \tag{2.77d}$$

where t^f are spike times and K is the number of spikes. $\theta(\dot{V}(t))$ ensures only positive values of $\dot{V}(t)$ are considered, so an absolute value sign is unnecessary. Calculating mean number of spikes (positive-slope threshold crossings) over the population requires taking the expectation value of N with respect to the density functional.

$$\langle N \rangle = \int_{-T/2}^{T/2} dt\ \langle\ \delta(V(t) - V_T)\ \dot{V}(t)\ \theta(\dot{V}(t))\ \rangle \tag{2.78a}$$

$$= \int_{-T/2}^{T/2} dt\ \ \nu_0 \tag{2.78b}$$

The LHS is expected number of spikes and the RHS is a time integral over some constant. In the $lim\ T \to 0$ this becomes an expression for overall population firing rate

$$\nu(t) = \langle\ \delta(V(t) - V_T)\ \dot{V}(t)\ \theta(\dot{V}(t))\ \rangle \tag{2.79}$$

which is now the rate of threshold crossings averaged over an ensemble. Note that $|\dot{V}(t)|$ in Eqn (2.77a) follows from a property of delta functions where $f(0) = 0$

$$\int_{-\infty}^{\infty} dt\ \delta(f(t)) = \int_{-\infty}^{\infty} dx\ \frac{1}{\dot{x}}\delta(x) = \frac{1}{|\dot{f}(0)|} \tag{2.80}$$

2.5.1 Stationary Firing Rate

For 'realistic' subthreshold statistics it is possible to calculate an exact analytic expression for population firing rate. The stationary firing rate is found with voltage fluctuations following a stationary Gaussian distribution. For calculation of the density

functional $P[\nu(t)]$ it is sufficient to know $P(V,\dot{V})$. Since the process is Gaussian all linear functionals are themselves Gaussian and for simplicity take $\langle V(t)\rangle = 0$.

$$P(V,\dot{V}) = \frac{1}{2\pi\underline{\underline{C}}} \exp\left(-\frac{1}{2}\begin{bmatrix} V \\ \dot{V}\end{bmatrix} \underline{\underline{C}}^{-1} \begin{bmatrix} V & \dot{V}\end{bmatrix}\right) \tag{2.81}$$

where $\underline{\underline{C}}$ is the diagonal *covariance matrix*

$$\underline{\underline{C}} = \begin{bmatrix} \langle V^2\rangle & \langle V\dot{V}\rangle \\ \langle \dot{V}V\rangle & \langle \dot{V}^2\rangle \end{bmatrix} = \begin{bmatrix} \sigma_V^2 & 0 \\ 0 & \sigma_{\dot{V}}^2 \end{bmatrix} \tag{2.82}$$

because off-diagonal elements vanish

$$\langle V\dot{V}\rangle = \langle \dot{V}V\rangle = \frac{1}{2}\frac{d}{dt}\langle V^2\rangle = 0 \tag{2.83}$$

which follows from the fact that for a stationary process a function and its derivative are independent. For a stationary process, density in terms of variances is given by

$$P(V,\dot{V}) = \frac{1}{2\pi\sigma_V\sigma_{\dot{V}}} \exp\left(-\frac{V^2}{2\sigma_V^2}\right) \exp\left(-\frac{\dot{V}^2}{2\sigma_{\dot{V}}^2}\right) \tag{2.84}$$

Calculation of the stationary firing rate is as follows

$$\begin{aligned}
\nu_0(t) &= \langle\ \dot{V}\delta(V - V_T)\theta(\dot{V})\ \rangle && \text{(2.85a)}\\
&= \int_{-\infty}^{\infty} dV \int_{-\infty}^{\infty} d\dot{V}\ \frac{1}{2\pi\sigma_V\sigma_{\dot{V}}}\delta(V-V_T)\theta(\dot{V})e^{-V^2/2\sigma_V^2}e^{-\dot{V}^2/2\sigma_{\dot{V}}^2} && \text{(2.85b)}\\
&= \int_{-\infty}^{\infty} dV \int_{0}^{\infty} d\dot{V}\ \frac{1}{2\pi\sigma_V\sigma_{\dot{V}}}\delta(V-V_T)e^{-V^2/2\sigma_V^2}e^{-\dot{V}^2/2\sigma_{\dot{V}}^2} && \text{(2.85c)}\\
&= \frac{e^{-V_T^2/2\sigma_V^2}}{2\pi\sigma_V\sigma_{\dot{V}}} \int_0^{\infty} d\dot{V}\ \dot{V}e^{-\dot{V}^2/2\sigma_{\dot{V}}^2} \qquad \because d\dot{V}\dot{V} = d\dot{V}^2/2 && \text{(2.85d)}\\
&= \frac{e^{-V_T^2/2\sigma_V^2}}{2\pi\sigma_V\sigma_{\dot{V}}} \int_0^{\infty} dx\ e^{-x/\sigma_{\dot{V}}^2} && \text{(2.85e)}\\
&= \frac{e^{-V_T^2/2\sigma_V^2}}{2\pi\sigma_V\sigma_{\dot{V}}}\sigma_{\dot{V}}^2 && \text{(2.85f)}\\
&= \frac{1}{2\pi}\frac{\sigma_{\dot{V}}}{\sigma_V}e^{-V_T^2/2\sigma_V^2} && \text{(2.85g)}
\end{aligned}$$

The term $\sigma_{\dot{V}}/\sigma_V$ has units of $[Hz]$ and its inverse is defined as the *differential correlation time*

$$\tau_c \equiv \left(\frac{\sigma_{\dot{V}}}{\sigma_V}\right)^{-1} \tag{2.86}$$

which is used to arrive at a final expression for stationary population firing rate

$$\nu_0(t) = \frac{1}{2\pi\tau_c} \exp\left[-\frac{1}{2}\left(\frac{V_T}{\sigma_V}\right)^2\right] \tag{2.87}$$

2.5.2 Covariance Function

The *covariance function*, for general functions termed *correlation*, gives the variance of the rate of change of a function with respect to itself. The covariance of membrane potential is

$$C_V(\tau) \equiv \langle V(t)V(t+\tau)\rangle \tag{2.88a}$$

$$\lim_{\tau\to 0} C_V(\tau) \longrightarrow \sigma_V^2 \tag{2.88b}$$

More precisely, membrane potential covariance is the expectation value of $V(t)$ evaluated at two separate times t_1, t_2

$$C_V(t_1, t_2) \equiv \langle V(t_1)V(t_2)\rangle \tag{2.89}$$

which can be used to calculate the covariance of $\dot{V}$ because

$$\frac{\partial}{\partial t_1}\frac{\partial}{\partial t_2} C_V(t_1, t_2) = \langle \dot{V}(t_1)\dot{V}(t_2)\rangle \tag{2.90}$$

For a stationary process covariance only depends on the *difference* τ between two time points , so taking $t_1 \to t_2$ gives

$$C_{\dot{V}}^2(0) = -\partial_\tau^2 C_V(\tau) \tag{2.91}$$

The correlation function must go to zero $C_V(\tau \to \pm\infty) \longrightarrow 0$. From Eqn (2.91) a second-derivative exists at $\tau = 0$. Therefore a second-order expansion around this point gives an inverted parabola centered at $C_V(0)$. The value at which this parabola reaches zero is twice the *differential correlation time* $2\tau_c$.

Knowledge of the correlation function $C_V(\tau)$ guarantees knowledge of all properties of a stationary random process. This is because any expectation value can be computed using $C(\tau)$. Of particular importance is *power spectral density* denoted S (to avoid confusion with probability density). Taking the Fourier transform of the covariance allows for direct calculation of

$$\tilde{C}_V(\omega) = S(\omega) = \langle \tilde{V}^2(\omega) \rangle \tag{2.92}$$

That is, the expectation value of Fourier transformed variance $\tilde{V}^2(\omega)$ is equal to power at each value of ω. Since Fourier coefficients are linear functions of $V(t)$ - which is Gaussian distributed - it follows that they too are Gaussian distributed.

$$\tilde{P}(\tilde{V}, \omega) = \frac{1}{2\pi S(\omega)} \exp\left[-\frac{\tilde{V}^2(\omega)}{2S(\omega)} \right] \tag{2.93}$$

The result that the Fourier transform of the covariance function equals power spectral density is mathematically explained by *Wiener-Khinchin theorem*; explicitly

$$S(\omega) = \frac{1}{\sqrt{2\pi}} \int_{-\infty}^{\infty} d\tau \; e^{i\omega t} C_V(\tau) \tag{2.94a}$$

$$C_V(\tau) = \frac{1}{\sqrt{2\pi}} \int_{-\infty}^{\infty} d\omega \; e^{-i\omega t} S(\omega) \tag{2.94b}$$

N.B. The Ornstein-Uhlenbeck process is a special limiting case in that it is smooth, but not twice differentiable at the origin. Therefore Eqn (2.92) does not strictly apply, but the results in general (*e.g.* Wiener-Khinchin theorem) do hold true.

2.5.3 Population Firing Rate

Beginning from the SDE for the general linear case

$$\tau_m \dot{V}(t) = -V + I_0(t) + \sigma\eta(t) \tag{2.95}$$

The equation of motion for the expectation value

$$\tau_m \langle \dot{V}(t) \rangle = \langle -V + I(t) + \sigma\eta(t) \tag{2.96a}$$

$$= -\langle V(t) \rangle + I_0(t) + \langle \sigma\eta(t) \rangle \tag{2.96b}$$

$$= -\langle V(t) \rangle + I_0(t) \tag{2.96c}$$

because the expectation value of the noise term is zero, $\langle \sigma\eta(t) \rangle = \sigma \langle \eta(t) \rangle = 0$. If the deterministic input current component $I_0(t)$ is a step input the ensemble average

$$\langle V(t) \rangle = \theta(t) e^{-t/\tau_m} \tag{2.97}$$

and a full expression for probability density is

$$P(V, \dot{V}, t) = \frac{1}{2\pi\sigma_V\sigma_{\dot{V}}} \exp\left(\frac{[V - \langle V(t) \rangle]^2}{2\sigma_V^2}\right) \exp\left(\frac{[\dot{V} - \langle \dot{V}(t) \rangle]^2}{2\sigma_{\dot{V}}^2}\right) \tag{2.98}$$

A closed form expression for population firing rate can now be calculated by expanding ν to first-order in small deviations around the mean to obtain

$$\nu(t) = \langle\ \dot{V}(t)\delta(V(t) - V_T)\theta(\dot{V})\ \rangle \tag{2.99a}$$

$$= \nu_0 \left(1 + \frac{V_T}{\sigma_V}\frac{\langle V(t) \rangle}{\sigma_V} + \sqrt{\frac{\pi}{2}}\frac{\langle \dot{V}(t) \rangle}{\sigma_{\dot{V}}}\right) \tag{2.99b}$$

The second term on the RHS is a *generator potential* component which means if input increases the difference between distribution mean and threshold becomes lower and firing rate is increased. The third term is proportional to membrane potential rate of change. Note that these expectation values are time dependent.

2.5.4 Linear Response Function

In the form of Eqn (2.99b) the Green's function in frequency representation can be directly inferred (after Fourier transforming)

$$\frac{\tilde{G}(\omega)}{\nu_0} = \frac{\tilde{\nu}_1(\omega)}{\nu_0} = \frac{V_T}{\sigma_V}\frac{\langle \tilde{V}(\omega) \rangle}{\sigma_V} + \sqrt{\frac{\pi}{2}}\frac{\langle \tilde{\dot{V}}(\omega) \rangle}{\sigma_{\dot{V}}} \tag{2.100}$$

where in the frequency domain $\tilde{G}(\omega)$ is termed a *frequency response function*. Since a Fourier transform of the first-derivative of a function is equal to $i\omega$ times the function this simplifies to

$$\frac{\tilde{\nu}_1(\omega)}{\nu_0} = \left(\frac{V_T}{\sigma_V^2} + \sqrt{\frac{\pi}{2}}\frac{i\omega}{\sigma_{\dot{V}}}\right)\langle\tilde{V}(\omega)\rangle \tag{2.101a}$$

$$= \left(\frac{V_T}{\sigma_V^2} + \sqrt{\frac{\pi}{2}}i\omega\tau_c\right)\langle\tilde{V}(\omega)\rangle \tag{2.101b}$$

$$= \left(\frac{V_T}{\sigma_V^2} + \sqrt{\frac{\pi}{2}}i\omega\tau_c\right)\frac{1}{1+i\omega\tau_m}\tilde{I}_0(\omega) \tag{2.101c}$$

$$\sim \frac{1+i\omega\tau_c}{1+i\omega\tau_m}\tilde{I}_0(\omega) \tag{2.101d}$$

$$\longrightarrow \frac{\tau_c}{\tau_m} \qquad \text{for } \omega \gg 1 \tag{2.101e}$$

The term outside brackets in Eqn (2.101c) represents time-dependent mean drive $I_0(t)$ being low-pass filtered into a spread out, temporally delayed $\tilde{I}_0(\omega)$. This causes a lagging population firing rate with typical timescale of the *membrane time constant* τ_m. Simultaneously current is being high-passed filtered with characteristic timescale given by the *correlation time constant* τ_c.

There are now two timescales and their ratio divides the dynamics into three qualitative types of behaviour. If $\tau_c < \tau_m$ there is signal attenuation as a function of increasing frequency. If $\tau_c > \tau_m$ signal boosting at high frequencies occurs. In the special case that $\tau_c = \tau_m$ there is perfect transmission at all frequencies.

Bibliography

[1] E. M. Itzhikevich, "Dynamical systems in neuroscience: The geometry of excitability and bursting," *The MIT Press*, (2006).

[2] P. Dayan and L. F. Abbott, "Theoretical neuroscience: Computational and mathematical modeling of neural systems," *The MIT Press*, (2001).

[3] W. Gerstner, W. M. Kistler, R. Naud, and L. Paninski, "Neuronal dynamics," *Cambridge University Press*, (2014).

[4] M. Cencini, F. Cecconi, and A. Vulpani, "Chaos: From simple models to complex dynamics," *World Scientific Publishing Co. Pte. Ltd.*, (2010).

[5] T. Tateno, A. Harsch, and H. Robinson, "Threshold firing frequency–current relationships of neurons in rat somatosensory cortex: Type 1 and type 2 dynamics," *Journal of Neurophysiology*, (2006).